Viscometric Functions for a Dilute Solution of Polymers in a Good Solvent

J. Ravi Prakash
Department of Chemical Engineering,
Indian Institute of Technology, Madras, India 600 036

Hans Christian Öttinger
Department of Materials, Institute of Polymers,
ETH Zürich, Zürich, Switzerland, CH-8092

February 1, 2008

Abstract

A dilute polymer solution is modeled as a suspension of non-interacting Hookean dumbbells and the effect of excluded volume is taken into account by incorporating a narrow Gaussian repulsive potential between the beads of each dumbbell. The narrow Gaussian potential is a means of regularising a delta-function potential—it tends to the delta-function potential in the limit of the width parameter μ going to zero. Exact predictions of viscometric functions in simple shear flow are obtained with the help of a retarded motion expansion and by Brownian dynamics simulations. It is shown that for relatively small *non-zero* values of μ, the presence of excluded volume causes a *swelling* of the dumbbell at equilibrium, and *shear thinning* in simple shear flow. On the other hand, a delta function excluded volume potential does not lead to either swelling or to shear thinning. Approximate viscometric functions, obtained by assuming that the bead-connector vector is described by a Gaussian non-equilibrium distribution function, are found to be accurate above a threshold value of μ, for a given value of the strength of excluded volume interaction, z. A first order perturbation expansion reveals that the Gaussian approximation is exact to first order in z. The predictions of an alternative quadratic excluded volume potential suggested earlier by Fixman (J. Chem. Phys., 1966, 45, 785; 793) are also compared with those of the narrow Gaussian potential.

1 Introduction

The fact that two parts of a polymer chain cannot occupy the same place at the same time due to their finite volume has been recognised in the polymer literature for many years now as being an extremely important microscopic phenomenon that governs the macroscopic behavior of polymer solutions.[7,8,20] Like hydrodynamic interaction, the *excluded volume* effect influences the properties of polymer solutions even in the limit of extremely long chains because it is responsible for segments remote from each other along the polymer chain interacting with each other.

While the effect of excluded volume on static properties of polymer solutions has been widely studied, there have been very few attempts at examining its influence on properties far from equilibrium. Excluded volume effects can be incorporated into bead-spring chain models for polymer solutions in a relatively straightforward manner by adding the excluded volume interaction force between a particular bead and all the other beads in the chain (pairwise) to the other potential forces that are acting on the bead. An noteworthy aspect of this approach is the kind of repulsive potential that is adopted to represent the excluded volume interactions. In static theories of polymer solutions, the excluded volume interaction is typically assumed to be a very short range δ-function potential.

Fixman[9] and more recently Ahn et al.[1] have attempted to predict the rheological properties of dilute polymer solutions by approximately incorporating the effects of both hydrodynamic interaction and excluded volume in a self-consistent manner into a bead-spring chain model. (Ahn et al. also include finitely extensible springs in place of Hookean springs). In order to obtain a solvable model, Fixman[9] used a repulsive quadratic excluded volume potential in place of a δ-function potential. This leads to a tractable model since the bead-connector vectors are then described by a Gaussian non-equilibrium distribution function. Results obtained with the quadratic excluded volume potential have, however, not been compared so far with the results of other models for the excluded volume potential.

Andrews et al.[2] have recently carried out a numerical study of the influence of excluded volume interactions on rheological and rheooptical properties of dilute solutions, with the help of Brownian dynamics and configuration biased Monte Carlo simulations. A bead-spring chain model, with "Fraenkel" springs between beads and a Morse potential to represent excluded volume interactions, was used to to model the flexible polymer molecule. Attention was largely confined to the prediction of properties in elongational flow and transient shear flow.

The predictions of their theories in the limit of long chains have not been considered by Fixman,[9] Ahn et al.[1] and Andrews et al.[2] On the other hand, the universal character of excluded volume effects have been studied using renormalisation group theory methods based on kinetic theory models (with a δ-function excluded volume potential) by Öttinger and coworkers.[14,23]

While the work of Andrews et al.[2] is based on Brownian Dynamics simulations, the accuracy of the other *approximate* treatments of excluded volume cited above

has not been tested by comparison with Brownian Dynamics simulations (which are an ideal tool for testing approximations for nonlinear effects). This is in contrast to the situation that exists for kinetic theory models that only incorporate hydrodynamic interaction effects, where extensive comparisons between the exact results of Brownian Dynamics simulations and various approximations have been made.[21,22]

It is the purpose of this paper to examine the influence of the excluded volume effect on the rheological properties of a dilute polymer solution by using a *narrow Gaussian potential* to describe the excluded volume interactions. Since the narrow Gaussian potential tends to the δ-function potential in the limit of a parameter μ (that describes the width of the potential) going to zero, it provides a means of evaluating results obtained with a singular δ-function potential. Compared to the δ-function potential, analytical calculations are not significantly harder with the narrow Gaussian potential; quite often, upon setting $\mu = 0$ at the end of a calculation, the predictions of a δ-function potential can be obtained. Furthermore, since Brownian dynamics simulations cannot be performed with a δ-function potential, simulations carried out with the narrow Gaussian potential for small values of the parameter μ provide a means of asymptotically obtaining the predictions of a δ-function potential model.

Any molecular theory that seeks to describe the dynamics of polymers in good solvents must simultaneously incorporate both the microscopic phenomena of hydrodynamic interaction and excluded volume, since hydrodynamic interaction effects have been shown to have an unavoidable influence on the dynamic behavior of polymer solutions. However, it would be difficult to explore the consequences of such a theory for two reasons. Firstly, the incorporation of hydrodynamic interaction would lead to the complication of multiplicative noise. Secondly, since Brownian dynamics simulations for long chains would be extremely computationally intensive, any approximations that are developed can only be tested for very short chains. For these reasons, and being in the nature of a preliminary investigation, we examine excluded volume effects independently from hydrodynamic interaction effects, and confine attention here to a Hookean dumbbell model for the polymer. This enables the careful evaluation of various approximations. It is hoped that, in the future, the best approximation can be used for chains with both hydrodynamic interaction and excluded volume, with the ultimate objective of calculating universal properties predicted in the long chain limit.

It must be noted that unlike in the case of the quadratic potential, the use of the narrow Gaussian potential does not lead to exact solvability. Indeed, as has been observed in earlier treatments of other non-linear microscopic phenomenon such as hydrodynamic interaction and internal viscosity, it is found that it is not possible to obtain an analytical solution valid at all shear rates. As a result, retarded motion expansions, Brownian dynamics simulations, and perturbative and non-perturbative approximation procedures are used in this work to obtain the material functions predicted by the narrow Gaussian potential.

An important consequence of using the narrow Gaussian potential is that the

nature of Fixman's quadratic excluded volume potential can be explored. Predictions of Fixman's quadratic excluded volume potential in simple shear flow will be compared with the predictions of the narrow Gaussian potential.

The outline of this paper is as follows. In section 2, the basic equations required to discuss the dynamics of Hookean dumbbells in good solvents are derived. In section 3, the various material functions considered in this paper are defined. A retarded motion expansion for the stress tensor, for arbitrary excluded volume potentials, is derived in section 4, and power series expansions for the material functions in simple shear flow are obtained. Section 5 is devoted to examining the consequences of describing the excluded volume interaction with a narrow Gaussian potential. In section 5.1, expressions for the material functions predicted with this potential at zero shear rate are obtained by using the retarded motion expansion. The formulation of a Brownian dynamics simulation algorithm is discussed in section 5.2, and a Gaussian approximation for the configurational distribution function is introduced in section 5.3. In section 5.4, a first order perturbation expansion in the strength of the excluded volume interaction is derived. Fixman's theory for dumbbells is presented in section 6, in terms of the framework adopted for the rest of the discussion in this paper. The results of the various exact and approximate treatments are compared and discussed in section 7, and the principal conclusions of the paper are summarised in section 8.

2 Basic Equations

The Hookean dumbbell model represents a macromolecule by a mechanical model that consists of two identical beads connected by a spring. The solvent in which the beads are suspended is assumed to be Newtonian, and attention is restricted to flows which have a homogeneous velocity field, *ie.* of the form $\boldsymbol{v} = \boldsymbol{v}_0 + \boldsymbol{\kappa}(t) \cdot \boldsymbol{r}$, where $\boldsymbol{v}_0$ is a constant vector, $\boldsymbol{\kappa}(t)$ is a traceless tensor, and $\boldsymbol{r}$ is the position vector with respect to a laboratory-fixed frame of reference. The instantaneous position of the beads are specified by bead position vectors $\boldsymbol{r}_1$ and $\boldsymbol{r}_2$.

This paper examines the consequence of introducing an excluded volume interaction between the beads of the dumbbell, so that the total potential experienced by the beads, ϕ, is the sum of the spring potential S, and the excluded volume potential E. The force on bead ν due to this potential, $\boldsymbol{F}_\nu^{(\phi)}$, is then given by $\boldsymbol{F}_\nu^{(\phi)} = -\partial\phi/\partial\boldsymbol{r}_\nu$. For Hookean springs, the spring potential is given by $S = (1/2)\,HQ^2$, where H is the spring constant. Two forms of the excluded volume potential are considered in this work, namely, the narrow Gaussian potential, and Fixman's quadratic potential. These are discussed in greater detail subsequently. Here, we summarise the governing equations that are valid for an arbitrary choice of the excluded volume potential E.

For homogeneous flows, the configurational distribution function $\psi(\boldsymbol{Q}, t)$ depends only on the internal configuration of the dumbbell, specified by the bead-connector

vector $\boldsymbol{Q} = \boldsymbol{r}_2 - \boldsymbol{r}_1$, and not on the center of mass. The quantity $\psi(\boldsymbol{Q}, t)\, d\boldsymbol{Q}$ is then the probability that at time t the dumbbell has a configuration in the range $\boldsymbol{Q}$ to $\boldsymbol{Q} + d\boldsymbol{Q}$. Using the framework of polymer kinetic theory[5] one can show that the distribution function $\psi(\boldsymbol{Q}, t)$, in the presence of excluded volume, satisfies the following *diffusion equation*,

$$\frac{\partial \psi}{\partial t} = -\frac{\partial}{\partial \boldsymbol{Q}} \cdot \left\{ (\boldsymbol{\kappa} \cdot \boldsymbol{Q})\, \psi - \frac{2}{\zeta}\, \psi\, \frac{\partial \phi}{\partial \boldsymbol{Q}} - \frac{2 k_B T}{\zeta}\, \frac{\partial \psi}{\partial \boldsymbol{Q}} \right\} \tag{1}$$

where, ζ is the bead friction coefficient (*ie.*, $\zeta = 6\pi\eta_s a$ for spherical beads with radius a, in a solvent with viscosity η_s), k_B is Boltzmann's constant, and T is the absolute temperature.

The stress tensor, $\boldsymbol{\tau}$, in a polymer solution is considered to be given by the sum of two contributions, $\boldsymbol{\tau} = \boldsymbol{\tau}^s + \boldsymbol{\tau}^p$, where $\boldsymbol{\tau}^s$ is the contribution from the solvent, and $\boldsymbol{\tau}^p$ is the polymer contribution. Since the solvent is assumed to be Newtonian, $\boldsymbol{\tau}^s = -\eta_s\, \dot{\boldsymbol{\gamma}}$, where $\dot{\boldsymbol{\gamma}}$ is the rate of strain tensor, $\dot{\boldsymbol{\gamma}} = (\nabla \boldsymbol{v})(t) + (\nabla \boldsymbol{v})^{\dagger}(t)$. The rheological properties of a dilute polymer solution may thus be obtained by calculating the polymer contribution to the stress tensor, $\boldsymbol{\tau}^p$. For a dumbbell model in the presence of excluded volume, it is given by the Kramer's expression,[5]

$$\boldsymbol{\tau}^p = -n \left\langle \boldsymbol{Q}\, \frac{\partial \phi}{\partial \boldsymbol{Q}} \right\rangle + n k_B T\, \mathbf{1} \tag{2}$$

Here, n is the number density of polymers, and angular brackets represent averaging with respect to the configurational distribution function $\psi(\boldsymbol{Q}, t)$.

For both the excluded volume potentials considered here, it will turn out that calculation of the second moment $\langle \boldsymbol{Q}\boldsymbol{Q} \rangle$ is necessary in order to evaluate the average in equation (2). A time evolution equation for the second moment can be obtained by multiplying the diffusion equation (1) by $\boldsymbol{Q}\boldsymbol{Q}$ and integrating over all configurations,

$$\frac{d}{dt} \langle \boldsymbol{Q}\boldsymbol{Q} \rangle = \boldsymbol{\kappa} \cdot \langle \boldsymbol{Q}\boldsymbol{Q} \rangle + \langle \boldsymbol{Q}\boldsymbol{Q} \rangle \cdot \boldsymbol{\kappa}^T + \frac{4 k_B T}{\zeta}\, \mathbf{1} - \frac{2}{\zeta} \left[\langle \boldsymbol{Q} \frac{\partial \phi}{\partial \boldsymbol{Q}} \rangle + \langle \frac{\partial \phi}{\partial \boldsymbol{Q}} \boldsymbol{Q} \rangle \right] \tag{3}$$

It proves convenient for subsequent calculations to introduce the following dimensionless variables,

$$t^* = \frac{t}{\lambda_H}, \quad \boldsymbol{Q}^* = \sqrt{\frac{H}{k_B T}}\, \boldsymbol{Q}, \quad \boldsymbol{\kappa}^* = \lambda_H \boldsymbol{\kappa}, \quad \phi^* = S^* + E^* \tag{4}$$

where, $\lambda_H = (\zeta / 4H)$ is the familiar time constant, $S^* = S / k_B T = (1/2)\, \boldsymbol{Q}^{*2}$ and $E^* = E / k_B T$ are the non-dimensional Hookean spring potential and the non-dimensional excluded volume potential, respectively. Note that θ-solvent values of a typical time scale (λ_H) and a typical length scale ($\sqrt{k_B T / H}$) are used for the purpose of non-dimensionalisation, regardless of the form of the excluded volume potential.

The intramolecular force is expected to be in the direction of the bead-connector vector. Therefore, it can be written in terms of non-dimensional variables as,

$$\frac{\partial \phi^*}{\partial \boldsymbol{Q}^*} = H^*(Q^*)\,\boldsymbol{Q}^* \tag{5}$$

where $H^*(Q^*)$ is an arbitrary function of the magnitude of $\boldsymbol{Q}^*$. As a result, the diffusion equation (1), in terms of non-dimensional variables, is given by,

$$\frac{\partial \psi}{\partial t^*} = -\frac{\partial}{\partial \boldsymbol{Q}^*} \cdot \left\{ \boldsymbol{\kappa}^* \cdot \boldsymbol{Q}^* - \frac{1}{2} H^*(Q^*)\,\boldsymbol{Q}^* \right\} \psi + \frac{1}{2} \frac{\partial}{\partial \boldsymbol{Q}^*} \cdot \frac{\partial \psi}{\partial \boldsymbol{Q}^*} \tag{6}$$

while, the Kramers expression (2) assumes the form,

$$\frac{\boldsymbol{\tau}^p}{n k_B T} = -\langle H^*(Q^*)\,\boldsymbol{Q}^* \boldsymbol{Q}^* \rangle + \mathbf{1} \tag{7}$$

and the second moment equation (3) becomes,

$$\frac{d}{dt^*} \langle \boldsymbol{Q}^* \boldsymbol{Q}^* \rangle = \boldsymbol{\kappa}^* \cdot \langle \boldsymbol{Q}^* \boldsymbol{Q}^* \rangle + \langle \boldsymbol{Q}^* \boldsymbol{Q}^* \rangle \cdot \boldsymbol{\kappa}^{*T} - \langle H^*(Q^*)\,\boldsymbol{Q}^* \boldsymbol{Q}^* \rangle + \mathbf{1} \tag{8}$$

Equation (8) is in general not a closed equation for the second moments since it depends on the form of the function $H^*(Q^*)$ (*ie.* on the choice of excluded volume potential).

On examining equations (7) and (8), it is straightforward to see that the second moment equation (8) is nothing but the Giesekus expression for the stress tensor,

$$\frac{\boldsymbol{\tau}^p}{n k_B T} = \frac{d}{dt^*} \langle \boldsymbol{Q}^* \boldsymbol{Q}^* \rangle - \boldsymbol{\kappa}^* \cdot \langle \boldsymbol{Q}^* \boldsymbol{Q}^* \rangle - \langle \boldsymbol{Q}^* \boldsymbol{Q}^* \rangle \cdot \boldsymbol{\kappa}^{*T} \tag{9}$$

While the equations derived in this section are valid for arbitrary homogeneous flows, in this paper we confine attention to the prediction of rheological properties in simple shear flows, defined in the section below.

3 Simple Shear Flows

3.1 Steady simple shear flow

Steady simple shear flows are described by a tensor $\boldsymbol{\kappa}$ which has the following matrix representation in the laboratory-fixed coordinate system,

$$\boldsymbol{\kappa} = \dot{\gamma} \begin{pmatrix} 0 & 1 & 0 \\ 0 & 0 & 0 \\ 0 & 0 & 0 \end{pmatrix} \tag{10}$$

where $\dot{\gamma}$ is the constant shear rate.

The three independent material functions used to characterize such flows are the viscosity, η_p, and the first and second normal stress difference coefficients, Ψ_1 and Ψ_2, respectively. These functions are defined by the following relations,[4]

$$\tau^p_{xy} = -\dot{\gamma}\,\eta_p\,; \qquad \tau^p_{xx} - \tau^p_{yy} = -\dot{\gamma}^2\,\Psi_1\,; \qquad \tau^p_{yy} - \tau^p_{zz} = -\dot{\gamma}^2\,\Psi_2 \tag{11}$$

3.2 Small amplitude oscillatory shear flow

A transient experiment that is used often to characterise polymer solutions is small amplitude oscillatory shear flow, where the tensor $\boldsymbol{\kappa}(t)$ is given by,

$$\boldsymbol{\kappa}(t) = \dot{\gamma}_0 \cos \omega t \begin{pmatrix} 0 & 1 & 0 \\ 0 & 0 & 0 \\ 0 & 0 & 0 \end{pmatrix} \tag{12}$$

Here, $\dot{\gamma}_0$ is the amplitude, and ω is the frequency of oscillations in the plane of flow. The polymer contribution to the shear stress, τ^p_{yx}, depends on time through the relation,[4]

$$\tau^p_{yx} = -\eta'(\omega)\, \dot{\gamma}_0 \cos \omega t - \eta''(\omega)\, \dot{\gamma}_0 \sin \omega t \tag{13}$$

where η' and η'' are the material functions characterising oscillatory shear flow. They are represented in a combined form as the complex viscosity, $\eta^* = \eta' - i\,\eta''$.

In the linear viscoelastic flow regime, the stress tensor is described by the linear constitutive relation,

$$\boldsymbol{\tau}^p(t) = -\int_{-\infty}^{t} ds\, G(t-s)\, \dot{\boldsymbol{\gamma}}(s) \tag{14}$$

where $G(t)$ is the relaxation modulus. As a result, for oscillatory shear flows with a small amplitude $\dot{\gamma}_0$, expressions for the real and imaginary parts of the complex viscosity can be found in terms of the relaxation modulus from the expression,

$$\eta^* = \int_0^\infty G(s)\, e^{-i\omega s}\, ds \tag{15}$$

Note that the zero shear rate viscosity $\eta_{p,0}$ and the zero shear rate first normal stress difference $\Psi_{1,0}$, which are linear viscoelastic properties, can be obtained from the complex viscosity in the limit of vanishing frequency,

$$\eta_{p,0} = \lim_{\omega \to 0} \eta'(\omega)\,; \qquad \Psi_{1,0} = \lim_{\omega \to 0} \frac{2\,\eta''(\omega)}{\omega} \tag{16}$$

4 Retarded Motion Expansion

A retarded motion expansion for the stress tensor, derived previously for the FENE dumbbell model,[5] can be adapted to the present instance by recognising that the FENE spring potential (as indeed any choice of excluded volume potential) is but a particular example of a connector force potential between the beads of the dumbbell. In this section, we briefly summarise the development of a retarded motion expansion for an arbitrary choice of the excluded volume potential. Details of the derivation may be found in Bird et al.[5]

We seek a solution of the diffusion equation (6) whereby the configurational distribution function, $\psi(\boldsymbol{Q}, t)$, can be written as a product of an equilibrium contribution and a flow contribution,

$$\psi(\boldsymbol{Q}, t) = \psi_{\text{eq}}(\boldsymbol{Q})\, \phi_{\text{fl}}\,(\boldsymbol{Q}, t) \tag{17}$$

The governing equation for the flow contribution $\phi_{\text{fl}}(\boldsymbol{Q}, t)$,

$$\frac{\partial \phi_{\text{fl}}}{\partial t^*} = -\left\{ \frac{\partial \phi_{\text{fl}}}{\partial \boldsymbol{Q}^*} - \phi_{\text{fl}} \frac{\partial \phi^*}{\partial \boldsymbol{Q}^*} \right\} \cdot \boldsymbol{\kappa}^* \cdot \boldsymbol{Q}^* + \frac{1}{2} \left\{ \frac{\partial}{\partial \boldsymbol{Q}^*} \cdot \frac{\partial \phi_{\text{fl}}}{\partial \boldsymbol{Q}^*} - \frac{\partial \phi_{\text{fl}}}{\partial \boldsymbol{Q}^*} \cdot \frac{\partial \phi^*}{\partial \boldsymbol{Q}^*} \right\} \tag{18}$$

can be obtained by substituting equation (17) into the diffusion equation (6), and exploiting the fact that the equilibrium distribution function is given by,

$$\psi_{\text{eq}}(\boldsymbol{Q}) = \mathcal{N}_{\text{eq}}\, e^{-\phi^*} \tag{19}$$

where $\mathcal{N}_{\text{eq}}$ is the normalisation constant.

Regardless of the form of the excluded volume potential, at steady state, an exact solution to equation (18) can be found for all homogeneous *potential* flows.[5] For more general homogeneous flows, however, it is necessary to seek a perturbative solution. The flow contribution, $\phi_{\text{fl}}(\boldsymbol{Q}, t)$, is assumed to be expandable in a power series in the velocity gradients,

$$\phi_{\text{fl}}(\boldsymbol{Q}, t) = 1 + \phi_1 + \phi_2 + \phi_3 + \ldots \tag{20}$$

where ϕ_k is of order k in the velocity gradient.

Partial differential equations governing each of the ϕ_k may be obtained by substituting equation (20) into equation (18) and equating terms of like order. Following the procedure suggested in Bird et al.,[5] one can judiciously guess the specific forms for the functions ϕ_k by noting that each of these functions must have certain properties. The form of the function ϕ_1 which satisfies these requirements is,

$$\phi_1 = \frac{1}{2}\, \boldsymbol{Q}^* \cdot \dot{\boldsymbol{\gamma}} \cdot \boldsymbol{Q}^* \tag{21}$$

while the form of ϕ_2 can be guessed to be,

$$\phi_2 = \frac{1}{8} (\boldsymbol{Q}^* \cdot \dot{\boldsymbol{\gamma}} \cdot \boldsymbol{Q}^*)^2 - \frac{1}{60} \langle\, \boldsymbol{Q}^{*4} \,\rangle_{\text{eq}}\, \text{tr}\, (\dot{\boldsymbol{\gamma}} \cdot \dot{\boldsymbol{\gamma}}) + A^*(Q^*)\, \boldsymbol{Q}^* \cdot \dot{\boldsymbol{\gamma}} \cdot \boldsymbol{\omega} \cdot \boldsymbol{Q}^* \tag{22}$$

where, $\langle \quad \rangle_{\text{eq}}$ denotes an average with $\psi_{\text{eq}}(\boldsymbol{Q})$, $\boldsymbol{\omega}$ is the vorticity tensor, defined here as $\boldsymbol{\omega} = \boldsymbol{\kappa}^* - \boldsymbol{\kappa}^{*T}$, and the scalar function $A^*(Q^*)$ obeys the following second order differential equation,

$$\frac{d^2 A^*}{d\, Q^{*2}} + \left(\frac{6}{Q^*} - H^*(Q^*)\, Q^* \right) \frac{d\, A^*}{d\, Q^*} - 2\, A^*(Q^*)\, H^*(Q^*) = 1 \tag{23}$$

It is difficult to suggest boundary conditions for equation (23) other than to say that the solution must be such that $\psi(\boldsymbol{Q}, t)$ is bounded. In the case of FENE springs, it is possible to explicitly obtain the particular solution of a similar second order differential equation.

It is clear from equation (9) that at steady state, the stress tensor can be found once $\langle \boldsymbol{Q}^* \boldsymbol{Q}^* \rangle$ is known. The second moment $\langle \boldsymbol{Q}^* \boldsymbol{Q}^* \rangle$ can be found correct to second

order in velocity gradients by using the power series expansion (20) for $\phi_{\rm fl}\left(\boldsymbol{Q},t\right)$, and the specific forms for ϕ_1 and ϕ_2 in equations (21) and (22), respectively. This leads to the following expression for the stress tensor, correct to third order in velocity gradients,

$$\begin{aligned}
-\frac{\boldsymbol{\tau}^p}{nk_BT} &= \frac{\lambda_H}{3}\left(\frac{H}{k_{\rm B}T}\right)\langle Q^2\rangle_{\rm eq}\{\dot{\boldsymbol{\gamma}}\}+\frac{\lambda_H^2}{30}\left(\frac{H}{k_{\rm B}T}\right)^2\langle Q^4\rangle_{\rm eq}\left\{2\dot{\boldsymbol{\gamma}}^2-(\dot{\boldsymbol{\gamma}}\cdot\boldsymbol{\omega}-\boldsymbol{\omega}\cdot\dot{\boldsymbol{\gamma}})\right\}\\
&+ \frac{\lambda_H^3}{105}\left(\frac{H}{k_{\rm B}T}\right)^3\langle Q^6\rangle_{\rm eq}\left\{\frac{3}{4}\,{\rm tr}\left(\dot{\boldsymbol{\gamma}}\cdot\dot{\boldsymbol{\gamma}}\right)\dot{\boldsymbol{\gamma}}-\frac{1}{2}\left(\dot{\boldsymbol{\gamma}}^2\cdot\boldsymbol{\omega}-\boldsymbol{\omega}\cdot\dot{\boldsymbol{\gamma}}^2\right)\right\}\\
&- \frac{\lambda_H^3}{180}\left(\frac{H}{k_{\rm B}T}\right)^3\langle Q^4\rangle_{\rm eq}\langle Q^2\rangle_{\rm eq}\left\{{\rm tr}\left(\dot{\boldsymbol{\gamma}}\cdot\dot{\boldsymbol{\gamma}}\right)\dot{\boldsymbol{\gamma}}\right\}\\
&+ \frac{\lambda_H^3}{30}\left(\frac{H}{k_{\rm B}T}\right)^2\langle Q^4\,A^*\rangle_{\rm eq}\left\{\left(\dot{\boldsymbol{\gamma}}^2\cdot\boldsymbol{\omega}-\boldsymbol{\omega}\cdot\dot{\boldsymbol{\gamma}}^2\right)+\boldsymbol{\omega}\cdot\left(\dot{\boldsymbol{\gamma}}\cdot\boldsymbol{\omega}-\boldsymbol{\omega}\cdot\dot{\boldsymbol{\gamma}}\right)\right.\\
&- \left.\left(\dot{\boldsymbol{\gamma}}\cdot\boldsymbol{\omega}-\boldsymbol{\omega}\cdot\dot{\boldsymbol{\gamma}}\right)\cdot\boldsymbol{\omega}\right\}+\ldots \qquad (24)
\end{aligned}$$

The Cayley-Hamilton theorem has been used to eliminate the term $\dot{\boldsymbol{\gamma}}^3$ in equation (24), and an isotropic term that does not affect the rheological properties has been dropped.

The stress tensor in simple shear flow, for small values of the non-dimensional shear rate $\lambda_H\,\dot{\gamma}$, can be found by substituting equation (10) for the rate of strain tensor, in equation (24). Using the definitions of the viscometric functions in equation (11), the following power series expansions are obtained,

$$\begin{aligned}
\frac{\eta_p}{\lambda_H nk_{\rm B}T} &= \frac{1}{3}\left(\frac{H}{k_{\rm B}T}\right)\langle Q^2\rangle_{\rm eq}+\left\{\frac{2}{15}\left(\frac{H}{k_{\rm B}T}\right)^2\langle Q^4\,A^*\rangle_{\rm eq}+\frac{1}{70}\left(\frac{H}{k_{\rm B}T}\right)^3\langle Q^6\rangle_{\rm eq}\right.\\
&- \left.\frac{1}{90}\left(\frac{H}{k_{\rm B}T}\right)^3\langle Q^4\rangle_{\rm eq}\langle Q^2\rangle_{\rm eq}\right\}(\lambda_H\,\dot{\gamma})^2+\ldots \qquad (25)\\
\frac{\Psi_1}{\lambda_H^2 nk_{\rm B}T} &= \frac{2}{15}\left(\frac{H}{k_{\rm B}T}\right)^2\langle Q^4\rangle_{\rm eq}+\ldots \qquad (26)
\end{aligned}$$

Clearly, equation (26) indicates that one must expand to higher orders in velocity gradients before the shear rate dependence of the first normal stress difference can be obtained. Zero shear rate properties, however, can be obtained from equations (25) and (26).

5 The Narrow Gaussian Potential

In the static theory of polymer solutions it is common to represent the dimensionless excluded volume potential, between two points on the polymer chain separated by a non-dimensional distance $\boldsymbol{Q}^*$, with the Dirac delta function,

$$E^*\left(\boldsymbol{Q}^*\right)=(2\pi)^{3/2}z\;\delta\left(\boldsymbol{Q}^*\right) \qquad (27)$$

where, $z = v\,(\,H/2\pi k_B T\,)^{3/2}$ is a non-dimensional parameter which represents the strength of the excluded volume interaction, and in which v—which has the dimensions of volume—is called the 'excluded volume parameter'.[8] The parameter z is frequently used in theories that incorporate excluded volume, as it is considered to be the appropriate parameter to be used in perturbation expansions. As mentioned earlier, excluded volume interactions are taken into account in this work by means of a narrow Gaussian potential.[15] The narrow Gaussian potential has the following form in terms of non-dimensional variables,

$$E^*\,(\boldsymbol{Q}^*) = \frac{z}{\mu^3}\;\exp\left(-\frac{1}{2}\,\frac{Q^{*2}}{\mu^2}\right) \tag{28}$$

It is clear from equation (28) that the non-dimensional parameter μ controls the extent of the excluded volume interaction, and as $\mu \to 0$, the narrow Gaussian potential tends to the δ–potential. The narrow Gaussian potential, as mentioned earlier, serves as a means of regularising the singular δ–potential and consequently, permits the evaluation of results obtained with a δ–potential.

With excluded volume interactions described by the narrow Gaussian potential, the function $H^*(Q^*)$, which appears in equation (5) for the non-dimensional force between the beads of the dumbbell, is given by,

$$H^*(Q^*) \equiv H_G^*(Q^*) = 1 - \left(\frac{z}{\mu^5}\right)\,\exp\left[-\frac{Q^{*2}}{2\mu^2}\right] \tag{29}$$

The complex form of this function implies that the diffusion equation (6) cannot be solved exactly analytically to obtain the non-equilibrium configurational distribution function $\psi(\boldsymbol{Q}, t)$. Furthermore, the time evolution equation for the second moments (8) is not a closed equation for the second moments since it involves the higher order moment $\langle H_G^*(Q^*)\,\boldsymbol{Q}^*\boldsymbol{Q}^*\rangle$ on the right hand side. As a result, perturbative methods, non-perturbative approximation procedures or numerical schemes must be used in order to obtain the material functions predicted by the narrow Gaussian potential.

5.1 Zero shear rate properties

The viscosity and the first normal stress difference predicted by the narrow Gaussian potential at low shear rates can be obtained from the equations (25) and (26), respectively, once the equilibrium averages that occur in these expressions are evaluated. For the narrow Gaussian potential, the equilibrium distribution function is given by equation (19), with the excluded volume contribution to the non-dimensional potential ϕ^* given by equation (28). We denote the various non-dimensional moments of the equilibrium distribution for a narrow Gaussian potential by,

$$q_m \equiv \left(\frac{H}{k_{\rm B}T}\right)^m \langle Q^{2m}\rangle_{\rm eq}\,; \quad m = 1, 2, 3, \ldots \tag{30}$$

In order to obtain the viscosity at non-zero shear rates, it is necessary to find the function A^* that satisfies the second order differential equation (23) [with $H^*(Q^*) = H^*_G(Q^*)$]. Unlike in the case of an FENE dumbbell, it has not been possible to obtain the particular solution to equation (23). As a result, attention is confined here to obtaining the zero shear rate predictions of the narrow Gaussian potential,

$$\frac{\eta_{p,0}}{\lambda_H n k_{\rm B} T} = \frac{1}{3}\, q_1 \tag{31}$$

$$\frac{\Psi_{1,0}}{\lambda_H^2 n k_{\rm B} T} = \frac{2}{15}\, q_2 \tag{32}$$

for which only the moments q_1 and q_2 are required. Alternative methods will be used in sections 5.2 to 5.4 to obtain the shear rate dependence of the viscometric functions.

The non-dimensional equilibrium moments q_1 and q_2 can be obtained exactly, as will be shown in section 5.1.1 below. The need to calculate equilibrium moments is also frequently encountered in static theories of polymer solutions. In these theories, as mentioned earlier, it is common to represent excluded volume interactions with a delta-function excluded volume potential, and furthermore, to obtain universal predictions by considering the limit of long chains. The Hamiltonian then typically has two singular objects—making it impossible to evaluate equilibrium moments exactly. The most succesful approach so far towards approximately evaluating these moments has been to develop a perturbation expansion in the parameter z, and to use renormalisation group methods to refine the results of the perturbation calculation.[7,8] An alternative and simpler non-perturbative route is the uniform expansion model.[8] The use of the narrow Gaussian potential—albeit in the simple context of Hookean dumbbells—provides an opportunity to compare the results of these approximate models with the exact solution. The rigorous solution is discussed in section 5.1.1 below, while the perturbation expansion and the uniform expansion models are discussed in sections 5.1.2 and 5.1.3, respectively.

5.1.1 Exact solution

It is straight forward to show that the moments q_m are given by the ratio of two integrals, $q_m = (I_m/I_0)$, where,

$$I_j \equiv \int_0^\infty Q^{*2j+2} \exp\{-(1/2)\, Q^{*2} - E^*\}\, dQ^*; \quad j = 0, 1, 2, \ldots \tag{33}$$

In the limit of $\mu \to 0$ and $\mu \to \infty$, these integrals can be evaluated analytically. Consider the quantities,

$$p_j(Q^*) \equiv Q^{*2j+2} \exp\{-\frac{1}{2}\, Q^{*2} - E^*\}$$

which are the integrands for the integrals I_j, and

$$R_j(Q^*) \equiv Q^{*2j+2} \exp\{-\frac{1}{2}\, Q^{*2}\}$$

Now, $p_j(0) = R_j(0) = 0$, for all values of μ. At any non-zero value of Q^*, it is clear from equation (28) that,

$$p_j(Q^*) \to R_j(Q^*) \quad \text{as} \quad \mu \to 0 \quad \text{or} \quad \infty$$

In other words, for all values of Q^*, the quantities $p_j(Q^*)$ tend *pointwise* to $R_j(Q^*)$ as μ tends to zero or to infinity. Furthermore, for all values of μ, it can be shown that $p_j(Q^*)$ are bounded functions of Q^* on $[0, \infty[$. It then follows from a theorem of the calculus[6] that,

$$q_m \to \frac{\int_0^\infty Q^{*2m+2} \exp\{-\frac{1}{2}Q^{*2}\}\, dQ^*}{\int_0^\infty Q^{*2} \exp\{-\frac{1}{2}Q^{*2}\}\, dQ^*} \quad \text{as} \quad \mu \to 0 \quad \text{or} \quad \infty$$

As a result, the asymptotic values of q_m for $\mu \to 0$ and $\mu \to \infty$ are found to be *independent* of z, and are equal to the θ-solvent values,

$$q_1 = 3\,; \quad q_2 = 15\,; \quad q_3 = 105\,; \ldots$$

This implies—from equations (31) and (32)—that the use of a delta-function potential to represent excluded volume interactions leads to the prediction of zero shear rate properties in good solvents which are identical to those in θ-solvents.

Away from these limiting values of μ, *i.e.* at non-zero finite values of μ, the integrals I_j can be found by numerical quadrature. Here they have been evaluated using a routine given in Numerical recipes[11] for the integration of an exponentially decaying integrand. Discussion of zero shear rate property predictions in this case is taken up in section 7.

5.1.2 Perturbation expansion

Static theories for polymer solutions indicate that accounting for excluded volume interactions with a delta function potential leads to the prediction of a *swelling* (*i.e.* an increase in the mean square end-to-end distance) of the polymer chain, which is in close agreement with experimental observations.[7,8] In the case of Hookean dumbbell, however, we have seen above that the use of a delta function potential to account for the presence of excluded volume (which corresponds to the limit $\mu \to 0$), does not lead to any change in the prediction of equilibrium moments when compared to the θ-solvent case. It is worthwhile therefore to examine the nature of the perturbation expansion in z, and to compare it with the results of the exact calculation.

Upon expanding e^{-E^*} in a power series, the integral I_j has the form,

$$I_j \equiv \int_0^\infty dQ^* \sum_{n=0}^{\infty} u_n(Q^*)\,; \quad j = 0, 1, 2, \ldots \tag{34}$$

where,

$$u_n(Q^*) = \frac{(-1)^n}{n!}\, Q^{*2j+2}\, e^{-\frac{1}{2}Q^{*2}}\, (\, E^*(Q^*)\,)^n \tag{35}$$

In order to carry out a term by term integration of the functional series $\sum_{n=0}^{\infty} u_n(Q^*)$ in equation (34), it is necessary for the series to be *uniformly convergent* on $[0, \infty[$. For all values of z, and $\mu \neq 0$, uniform convergence can be established with the help of the Weierstrass M test.[6] Therefore, a term by term integration in equation (34) can be caried out, *except* when $\mu = 0$. Assuming that $\mu \neq 0$, and performing the integration in equation (34), one obtains,

$$I_j = 2^{j+\frac{1}{2}}\,\Gamma\Big(j+\frac{3}{2}\Big)\,\sum_{n=0}^{\infty}\,\frac{(-1)^n}{n!}\Big(\frac{z}{\mu^3}\Big)^n\,\frac{\mu^{2j+3}}{(n+\mu^2)^{j+\frac{3}{2}}};\quad j=0,1,2,\ldots \tag{36}$$

Consider the moment q_1, which is undoubtedly the most interesting physical moment. Using the perturbation expansion for I_j, q_1 is given by the ratio, $q_1 = 3\,(S_1/S_0)$, where, S_0 and S_1 are defined by,

$$\begin{aligned} S_0 &= \sum_{n=0}^{\infty}\,\frac{(-1)^n}{n!}\Big(\frac{z}{\mu^3}\Big)^n\,\frac{\mu^3}{(n+\mu^2)^{\frac{3}{2}}} \\ S_1 &= \sum_{n=0}^{\infty}\,\frac{(-1)^n}{n!}\Big(\frac{z}{\mu^3}\Big)^n\,\frac{\mu^5}{(n+\mu^2)^{\frac{5}{2}}} \end{aligned} \tag{37}$$

If only the first order perturbation term is retained, one obtains,

$$q_1 = 3\,\left(1+\frac{z}{(1+\mu^2)^{5/2}}\right) \tag{38}$$

Curiously, the limit $\mu \to 0$ can be carried out in this case. It leads to a result which is in line with static theories, which indicate a finite non-vanishing effect due to the presence of δ-potential excluded volume interactions. However, such a limit cannot be carried out if higher order terms are retained, since both the sums S_0 and S_1 diverge as $\mu \to 0$. In static theories, higher order perturbation expansions are obtained by *dropping* divergent terms, as they are postulated not to matter. These divergent terms arise from products of the δ-potential for the *same* pair of interacting beads. In dumbbells, these are the only kind of beads present. As a result, there is no meaningful or mathematically consistent way of going beyond first order perturbation theory for dumbells in the limit $\mu \to 0$.

Note that both the series, S_0 and S_1, are alternating series. Furthermore, for given values of z and μ, the terms decrease monotonically for large enough values of n. It follows then, from the Leibnitz criterion for alternating series,[3] that both S_0 and S_1 converge for all values of z and $\mu \neq 0$. This suggests that, even though it is not possible to switch the integral and summation in equation (34) for $\mu = 0$, the value of q_1 at $\mu = 0$ can be found by setting it equal to the limit of $q_1(\mu)$ as $\mu \to 0$. We shall see in section 7 that such a limiting process is infeasible since it becomes numerically impossible to evaluate the sums (37) for small enough values of μ.

5.1.3 Uniform expansion model

The uniform expansion model seeks to approximate the average $\langle X \rangle_{\rm eq}$ of any quantity $X(\boldsymbol{Q})$, with $\langle X \rangle'_{\rm eq}$, where $\langle \quad \rangle'_{\rm eq}$ denotes an average with the Gaussian equilibrium distribution function,

$$\psi'_{\rm eq}(\boldsymbol{Q}) = \mathcal{N}'_{\rm eq} \exp\{ -\frac{3}{2b'^2} Q^2 \} \tag{39}$$

with $\mathcal{N}'_{\rm eq} = [\, 3/2\pi b'^2 \,]^{3/2}$. The aim is to find the parameter b' that leads to the best possible approximation. As may be expected, this depends on the quantity $X(\boldsymbol{Q})$ that is averaged. The motivation behind the uniform expansion model, and details regarding the calculation of b' are given in appendix A. Since the equilibrium distribution function in the absence of excluded volume is Gaussian, this assumption expects the equilibrium distribution to remain Gaussian upon the incorporation of excluded volume, albeit with an increased end-to-end vector.

If we define u_m, such that $u_m \equiv (H/k_{\rm B}T)^m \langle Q^{2m} \rangle'_{\rm eq}$, then clearly u_m is the uniform expansion model approximation for q_m. The uniform expansion model predictions of the zero shear rate properties are given by (31) and (32), with q_m replaced by u_m. Results of material properties obtained by numerical quadrature, and by the uniform expansion model, are discussed in section 7.

5.2 Brownian dynamics simulations

Development of the retarded motion expansion has proved useful in obtaining exact expressions for the zero shear rate properties. At non-zero shear rates, exact predictions of the viscometric functions can be obtained by solving the Ito stochastic differential equation,

$$d\boldsymbol{Q}^* = \left[\boldsymbol{\kappa}^* - \frac{1}{2} H^*(Q^*)\, \mathbf{1} \right] \cdot \boldsymbol{Q}^*\, dt + d\boldsymbol{W} \tag{40}$$

which corresponds to the non-dimensional diffusion equation (6), and in which $\boldsymbol{W}$ is a three-dimensional Wiener process.

For the narrow Gaussian potential, since $H^*(Q^*) = H^*_G(Q^*)$, equation (40) is non-linear. As a result, it cannot be solved analytically. Two different Brownian dynamics simulation algorithms have been adopted here for the numerical solution of equation (40). Both schemes use a second order predictor-corrector algorithm with time-step extrapolation.[15] The first scheme obtains steady-state expectations by the simulation of a single long trajectory, and is based on the assumption of ergodicity.[15] It has been used to obtain results at equilibrium, and for large values of the shear rate. A second algorithm—which employs a variance reduction procedure—has been used at low values of the shear rate, since the variance for the viscometric functions is found to be relatively large at these shear rates. Reduction in the variance is obtained by following a scheme suggested by Wagner and

Öttinger.[18] The scheme—which constructs an ensemble of trajectories over several relaxation times, from start-up of flow to steady-state—essentially consists of subtracting the rheological properties obtained from a parallel equilibrium simulation. While this doesn't change the average values of the properties, it significantly reduces the fluctuations, since the fluctuations are virtually the same at zero and small shear rates. The results of these simulation algorithms are discussed in section 7.

5.3 The Gaussian approximation

The main obstacle (in the configuration space of the dumbbell) to obtaining the rheological properties predicted by a narrow Gaussian potential is that the second moment equation is not a closed equation. A closure problem has also been encountered earlier in treatments of the phenomenon of hydrodynamic interaction and internal viscosity, where it has been shown that an accurate approximation can be obtained by assuming that the non-equilibrium configurational distribution function is a Gaussian distribution.[16,17,19,21,22] In this section, a similar systematic approximation procedure for the treatment of excluded volume interactions described by a narrow Gaussian potential is introduced.

The assumption that $\psi(\boldsymbol{Q},t)$ is a Gaussian distribution,

$$\psi(\boldsymbol{Q},t)=\frac{1}{(2\pi)^{3/2}}\,\frac{1}{\sqrt{\det\langle\boldsymbol{QQ}\rangle}}\;\exp\left\{-\frac{1}{2}\,\boldsymbol{Q}\cdot\langle\boldsymbol{QQ}\rangle^{-1}\cdot\boldsymbol{Q}\right\} \tag{41}$$

makes the second moment equation (8) a closed equation, since the higher order moment $\langle H_G^*(Q^*)\,\boldsymbol{Q}^*\boldsymbol{Q}^*\rangle$ can be expressed in terms of the second moment. On performing this reduction, it can be shown that the Gaussian approximation leads to the following closed second moment equation,

$$\frac{d}{dt^*}\langle\boldsymbol{Q}^*\boldsymbol{Q}^*\rangle=\boldsymbol{\kappa}^*\cdot\langle\boldsymbol{Q}^*\boldsymbol{Q}^*\rangle+\langle\boldsymbol{Q}^*\boldsymbol{Q}^*\rangle\cdot\boldsymbol{\kappa}^{*T}-\langle\boldsymbol{Q}^*\boldsymbol{Q}^*\rangle+\frac{z}{\sqrt{\det\left[\,\langle\boldsymbol{Q}^*\boldsymbol{Q}^*\rangle+\,\mu^2\,\mathbf{1}\right]}}\,\boldsymbol{\Pi}+\mathbf{1} \tag{42}$$

where,

$$\boldsymbol{\Pi}=\left[\langle\boldsymbol{Q}^*\boldsymbol{Q}^*\rangle+\mu^2\,\mathbf{1}\,\right]^{-1}\cdot\langle\boldsymbol{Q}^*\boldsymbol{Q}^*\rangle$$

It is also straight forward to show that on introducing the Gaussian approximation, the Giesekus expression for the stress tensor has the form,

$$\frac{\boldsymbol{\tau}^p}{nk_BT}=-\langle\boldsymbol{Q}^*\boldsymbol{Q}^*\rangle+\frac{z}{\sqrt{\det\left[\,\langle\boldsymbol{Q}^*\boldsymbol{Q}^*\rangle+\,\mu^2\,\mathbf{1}\right]}}\,\boldsymbol{\Pi}+\,\mathbf{1} \tag{43}$$

The steady state viscometric functions [defined by equations (11)] can therefore be found once equation (42) is solved for $\langle\boldsymbol{Q}^*\boldsymbol{Q}^*\rangle$.

It is worth examining the nature of the polymer contribution to the stress tensor. In the limit $\mu\to 0$, $\boldsymbol{\Pi}$ reduces to $\mathbf{1}$, and as a result, the presence of excluded volume

only makes an indirect contribution through its influence on the second moment $\langle \boldsymbol{Q}^*\boldsymbol{Q}^*\rangle$. This follows from the fact that an isotropic contribution to the stress tensor makes no difference to the rheological properties of the polymer solution. On the other hand, for non-zero values of μ, the rheological properties are also affected directly by excluded volume.

Under the Gausssian approximation, linear viscoelastic properties can be obtained by deriving a first order codeformational memory integral expansion for the stress tensor. The tensor $\langle \boldsymbol{Q}^*\boldsymbol{Q}^*\rangle$ is expanded, in terms of deviations from its isotropic equilibrium solution, upto first order in velocity gradient,

$$\langle \boldsymbol{Q}^*\boldsymbol{Q}^*\rangle = \alpha^2\,(\mathbf{1} + \boldsymbol{\epsilon} + \dots) \tag{44}$$

where, the parameter α (commonly called the swelling ratio) is defined by,

$$\alpha^2 = \frac{\langle\, Q^2\,\rangle_{\rm eq}}{\langle\, Q^2\,\rangle_{0,\rm eq}} \tag{45}$$

Here, $\langle\, Q^2\,\rangle_{0,\rm eq} = (3k_BT/H)$, is the mean square end-to-end distance in the absence of excluded volume. Clearly, α represents the *equilibrium* swelling of the polymer chain caused by the presence of excluded volume. α is not an independent parameter since at equilibrium the second moment equation (42) reduces to the following consistency relationship between z, μ and α,

$$z = (1-\alpha^{-2})\,[\,\alpha^2+\mu^2\,]^{\frac{5}{2}} \tag{46}$$

The well known scaling relation for the end-to-end distance with the number of monomers N, namely, $\sqrt{\langle\, Q^2\,\rangle_{\rm eq}} \sim N^{3/5}$, may be obtained from equations (45) and (46) in the limit of large N by noting that—since excluded volume is a pairwise interaction—z must scale as $\sqrt{N}$ for dumbbells.[10]

Substituting the expansion (44) into the evolution equation (42) leads to,

$$\frac{d}{dt^*}\,\boldsymbol{\epsilon} = \boldsymbol{\kappa}^* + \boldsymbol{\kappa}^{*T} - \frac{1}{\tau^*}\,\boldsymbol{\epsilon} \tag{47}$$

where,

$$\tau^* = \left[1 - \frac{z\,\mu^2}{(\,\alpha^2+\mu^2\,)^{7/2}}\right]^{-1} \tag{48}$$

Furthermore, the stress tensor (43) upto first order in the velocity gradient (without the rheologically unimportant isotropic contribution) is given by,

$$\frac{\boldsymbol{\tau}^p}{nk_BT} = -\mathcal{H}\,\boldsymbol{\epsilon} \tag{49}$$

where,

$$\mathcal{H} = \alpha^2\,(\tau^*)^{-1} \tag{50}$$

Upon integrating equation (47), which is a first order ordinary differential equation for $\boldsymbol{\epsilon}$, and substituting the result into equation (49), the following codeformational integral expansion is obtained,

$$\boldsymbol{\tau}^p(t) = -\int_{-\infty}^{t} ds\, nk_BT\, \tilde{G}(t-s)\, \boldsymbol{\gamma}_{[1]}(t,s) \tag{51}$$

where $\boldsymbol{\gamma}_{[1]}$ is the codeformational rate-of-strain tensor[4] and the memory function $\tilde{G}(t)$ is given by

$$\tilde{G}(t) = \mathcal{H}\, e^{-(t/\lambda_H \tau^*)} \tag{52}$$

The product $\lambda_H \tau^*$ is usually interpreted as a relaxation time, and $\mathcal{H}$ as a relaxation weight. Clearly, the incorporation of excluded volume effects increases the relaxation time in a good solvent relative to a theta solvent by a factor of τ^*.

The memory function $\tilde{G}(t)$ can now be used to derive the linear viscoelastic material properties. Substituting $G(t) = nk_BT\tilde{G}(t)$, into equation (15), leads to,

$$\frac{\eta'(\omega)}{\lambda_H nk_BT} = \frac{\tau^*\,\mathcal{H}}{1+(\lambda_H\tau^*\,\omega)^2} \quad ; \quad \frac{\eta''(\omega)}{\lambda_H^2 nk_BT} = \frac{\omega\,\tau^{*2}\,\mathcal{H}}{1+(\lambda_H\tau^*\,\omega)^2} \tag{53}$$

Upon taking the limit of $\omega \to 0$ we obtain,

$$\frac{\eta_{p,0}}{\lambda_H nk_BT} = \tau^*\,\mathcal{H} \quad ; \quad \frac{\Psi_{1,0}}{\lambda_H^2 nk_BT} = 2\,\tau^{*2}\,\mathcal{H} \tag{54}$$

At moderate to large values of the shear rate, it is not possible to obtain analytical expressions for the shear rate dependence of the viscometric functions, and consequently a numerical procedure is required. Since the second moment $\langle \boldsymbol{Q}^*\boldsymbol{Q}^* \rangle$ shares the symmetry of the flow field in simple shear flow, its Cartesian components can be denoted by,

$$\langle \boldsymbol{Q}^*\boldsymbol{Q}^* \rangle = \begin{pmatrix} s_1 & s_4 & 0 \\ s_4 & s_2 & 0 \\ 0 & 0 & s_3 \end{pmatrix} \tag{55}$$

Upon substituting equation (55) into equation (42), a system of four first order ordinary differential equations for the quantities s_j, $j = 1, \ldots, 4$ is obtained. Steady state viscometric functions, as functions of shear rate, can then be found by numerically integrating these equations with respect to time (using a simple Euler scheme) until steady state is reached. Results obtained by this procedure are discussed in section 7.

5.4 First order perturbation expansion in z

The influence of excluded volume effects on the universal shear rate dependence of viscometric functions has been studied, as mentioned earlier, by using renormalisation group methods.[14,23] The renormalisation group theory approach is essentially

a method for refining the results of a low order perturbation expansion in z, by introducing higher order interactions effects so as to remove the ambiguous definition of the bead size. Results of this approach, based on a δ-function excluded volume potential, indicate that the presence of excluded volume has a non-trivial influence on the shear rate dependence of the viscometric functions. We have seen earlier in this work that as far as equlibrium swelling and zero shear rate properties are concerned, the use of a δ-function excluded volume potential leads to trivial results. In this section, a first order perturbation expansion in z—with a narrow Gaussian excluded volume potential—is constructed, in order to compare its predictions of shear rate dependence with those obtained with Brownian dynamics simulations, and with the Gaussian approximation. The dependence of the predictions on the width parameter μ is of particular interest.

A first order perturbation expansion can be constructed, following the procedure suggested in references,[13,14] from the second moment equation (8). We assume that the configurational distribution function ψ can be written as $\psi_\theta + \psi_z$, where ψ_θ is the distribution function in the absence of excluded volume, i.e. in a θ-solvent, and ψ_z is the correction to first order in the strength of the excluded volume interaction. The averages performed with these contributions will be denoted by $\langle \cdots \rangle_\theta$ and $\langle \cdots \rangle_z$, respectively.

On equating terms of equal order, equation (8) can be rewritten as two equations, namely, a zeroth order second moment equation and a first order second moment equation. The zeroth order equation—which is linear in the moment $\langle \boldsymbol{Q}^*\boldsymbol{Q}^* \rangle_\theta$—is the well known second moment equation for Hookean dumbbells in a θ-solvent.[5] It has the analytical solution,[5]

$$\langle \boldsymbol{Q}^*\boldsymbol{Q}^* \rangle_\theta = \mathbf{1} - \int_{-\infty}^{t^*} ds^*\, e^{-(t^*-s^*)}\, \boldsymbol{\gamma}_{[0]}(t^*, s^*) \tag{56}$$

where, $\boldsymbol{\gamma}_{[0]}$ is the codeformational relative strain tensor.[4] The first order second moment equation has the form,

$$\frac{d}{dt^*}\langle \boldsymbol{Q}^*\boldsymbol{Q}^* \rangle_z = \boldsymbol{\kappa}^* \cdot \langle \boldsymbol{Q}^*\boldsymbol{Q}^* \rangle_z + \langle \boldsymbol{Q}^*\boldsymbol{Q}^* \rangle_z \cdot \boldsymbol{\kappa}^{*T} - \langle \boldsymbol{Q}^*\boldsymbol{Q}^* \rangle_z + \frac{z}{\mu^5} \langle e^{-(Q^{*2}/2\mu^2)}\, \boldsymbol{Q}^*\boldsymbol{Q}^* \rangle_\theta \tag{57}$$

The θ-solvent distribution function ψ_θ is a Gaussian,[5] and consequently, the complex moment on the right hand side of equation (57) can be reduced to a function of $\langle \boldsymbol{Q}^*\boldsymbol{Q}^* \rangle_\theta$. The following equation is obtained on performing this reduction,

$$\frac{d}{dt^*}\langle \boldsymbol{Q}^*\boldsymbol{Q}^* \rangle_z = \boldsymbol{\kappa}^* \cdot \langle \boldsymbol{Q}^*\boldsymbol{Q}^* \rangle_z + \langle \boldsymbol{Q}^*\boldsymbol{Q}^* \rangle_z \cdot \boldsymbol{\kappa}^{*T} - \langle \boldsymbol{Q}^*\boldsymbol{Q}^* \rangle_z + \boldsymbol{Y} \tag{58}$$

where,

$$\boldsymbol{Y} = \frac{z}{\sqrt{\det\left[\, \langle \boldsymbol{Q}^*\boldsymbol{Q}^* \rangle_\theta + \mu^2\, \mathbf{1} \right]}} \left[\langle \boldsymbol{Q}^*\boldsymbol{Q}^* \rangle_\theta + \mu^2\, \mathbf{1} \,\right]^{-1} \cdot \langle \boldsymbol{Q}^*\boldsymbol{Q}^* \rangle_\theta$$

Clearly, equation (58) could have also been derived by expanding the second moment equation for the Gaussian approximation (42) to first order in z. It follows,

therefore, that the Gaussian approximation is exact to first order in z. This is also the situation in the case of the Gaussian approximation introduced for the treatment of hydrodynamic interaction effects, where it was found to be exact to first order in the strength of hydrodynamic interaction, h^*.[13]

Equation (58) is a system of linear inhomogeneous ordinary differential equations, whose solution is,

$$\langle \boldsymbol{Q}^*\boldsymbol{Q}^* \rangle_z = \int_{-\infty}^{t^*} ds^*\, e^{-(t^*-s^*)}\, \boldsymbol{E}(t^*,s^*)\cdot\boldsymbol{Y}\cdot\boldsymbol{E}^T(t^*,s^*) \tag{59}$$

where, $\boldsymbol{E}$ is the displacement gradient tensor.[4]

The expression for the stress tensor (7) can also be expanded to first order in z. After reduction of complex moments to second moments, the stress tensor depends only on the second moments $\langle \boldsymbol{Q}^*\boldsymbol{Q}^* \rangle_\theta$ and $\langle \boldsymbol{Q}^*\boldsymbol{Q}^* \rangle_z$. Equations (56) and (59) may then be used to derive the following first order perturbation theory expression for the stress tensor in arbitrary homogeneous flows,

$$\frac{\boldsymbol{\tau}^p}{nk_BT} = \boldsymbol{Y} + \int_{-\infty}^{t^*} ds^*\, e^{-(t^*-s^*)}\, \Big(\boldsymbol{\gamma}_{[0]}(t^*,s^*) - \boldsymbol{E}(t^*,s^*)\cdot\boldsymbol{Y}\cdot\boldsymbol{E}^T(t^*,s^*)\Big) \tag{60}$$

Note that $\boldsymbol{Y}$, the direct contribution to the stress tensor, is isotropic only in the limit $\mu \to 0$.

The form in steady shear flow, of the tensors $\boldsymbol{\gamma}_{[0]}$ and $\boldsymbol{E}$, has been tabulated in reference.[4] Using the expression for the stress tensor (60), and the definition of the viscometric functions (11), the following first order perturbation theory results for the viscometric functions are obtained,

$$\frac{\eta_p}{\lambda_H n k_{\rm B} T} = 1 + \left(\frac{1+\mu^2+\lambda_H^2\dot\gamma^2}{\sqrt{1+\mu^2}\,\Delta^{3/2}}\right) z \tag{61}$$

$$\frac{\Psi_1}{\lambda_H^2 n k_{\rm B} T} = 2 + 2\left(\frac{1+2\,\mu^2+\lambda_H^2\dot\gamma^2}{\sqrt{1+\mu^2}\,\Delta^{3/2}}\right) z \tag{62}$$

where, $\Delta = (1+\mu^2)[1+\mu^2+2\lambda_H^2\dot\gamma^2] - \lambda_H^2\dot\gamma^2$. In the limit of $\lambda_H\dot\gamma$ going to zero, the expression for the viscosity (61) reduces to the expression derived earlier in section 5.1—using the retarded motion expansion and the equilibrium perturbation expansion—for the zero shear rate viscosity. One can also show that $\mathrm{tr}\langle \boldsymbol{Q}^*\boldsymbol{Q}^* \rangle$ reduces to the equilibrium moment q_1 [see equation (38)], in the limit $\lambda_H\dot\gamma \to 0$.

The first order perturbation results are compared with simulation results, and with results of the Guassian approximation, in section 7.

6 Fixman's Theory

Many years ago, in path-breaking seminal work, Fixman[9] considered the simultaneous inclusion of hydrodynamic interaction and excluded volume in bead-spring

chain models for dilute polymer solutions. In order to render the problem solvable, Fixman introduced a number of approximations. Since we are only concerned with excluded volume in the context of Hookean dumbbells in this work, we shall only consider those approximations which are relevant in this context. The introduction of the quadratic potential, the governing equations of Fixman's theory, and the calculation of material functions predicted by the theory in simple shear flow are considered in this section.

6.1 The quadratic potential

With regard to excluded volume, the most crucial approximation of Fixman[9] is the replacement of the delta function potential with a quadratic potential. By adopting a Boson operator formulation of the governing equations, Fixman has shown that the delta function potential (27) may be represented by,

$$E^*\left(\boldsymbol{Q}^*\right) = \frac{1}{2}\,\boldsymbol{Q}^* \cdot \boldsymbol{G}^* \cdot \boldsymbol{Q}^* \tag{63}$$

where $\boldsymbol{G}^*$ is a symmetric function of various configuration dependent quantities introduced in the Boson operator formalism. From this expression it is clear that a quadratic potential for the excluded volume may be obtained by replacing the fluctuating quantity $\boldsymbol{G}^*$ with an average. Fixman obtains a quadratic potential by replacing $\boldsymbol{G}^*$ with a configuration dependent average, as described below.

As a result of replacing $\boldsymbol{G}^*$ with its average, one can show from equation (63) that,

$$\langle\, \boldsymbol{G}^* \,\rangle = \langle\, \frac{\partial}{\partial \boldsymbol{Q}^*}\, \frac{\partial E^*}{\partial \boldsymbol{Q}^*} \,\rangle \tag{64}$$

In other words, for any given potential E^*, one can find $\langle\, \boldsymbol{G}^* \,\rangle$ provided that the non-equilibrium distribution function $\psi(\boldsymbol{Q}, t)$ with which to carry out the average on the right hand side of equation (64) is known. It turns out that $\psi(\boldsymbol{Q}, t)$, in the presence of a quadratic excluded volume potential and with consistently averaged hydrodynamic interaction,[12,16] is a Gaussian distribution. Evaluation of the average for a δ–potential (27), with a Gaussian distribution (41), leads to the following non-dimensional quadratic potential,

$$E^*\left(\boldsymbol{Q}^*\right) = -\frac{1}{2}\,\frac{z}{\sqrt{\det\langle \boldsymbol{Q}^*\boldsymbol{Q}^*\rangle}}\;\boldsymbol{Q}^* \cdot \langle \boldsymbol{Q}^*\boldsymbol{Q}^*\rangle^{-1} \cdot \boldsymbol{Q}^* \tag{65}$$

It is straightforward to show that the potential (65) leads to an unphysical *non-central* excluded volume force between the beads. Fixman, perhaps for this reason, introduces a further approximation which consists of replacing the above potential with the following simpler form,

$$E^*\left(\boldsymbol{Q}^*\right) = -\frac{1}{2}\,\frac{z}{\alpha^2}\,\frac{Q^{*2}}{\sqrt{\det\langle \boldsymbol{Q}^*\boldsymbol{Q}^*\rangle}} \tag{66}$$

where, α is defined as before by equation (45). However, in this case, α obeys the consistency relation,

$$z = (\,\alpha^2 - 1)\,\alpha^3 \tag{67}$$

Interestingly enough, equation (46) reduces to equation (67) in the limit $\mu \to 0$ (which corresponds to a δ–potential).

It is appropriate here to note that while Fixman has presented all his arguments for bead-spring chain models, the form of Fixman's potential for dumbbells given above can be found in the book by Larson.[10]

The consequences of adopting the quadratic excluded volume potential (66) are briefly discussed in the following section. It is worthwhile to point out here that Fixman's original formulation of the problem was not in terms of the Gaussian distributions and second moments discussed below. Rather, his attempt was to directly solve the diffusion equation (1) for the configurational distribution function, and then carry out the average in equation (2) to obtain the rheological properties. It is, however, possible to discuss his approach within the framework developed subsequently by Öttinger[12] and this is the procedure that is adopted here. A graphic exposition of Fixman's algorithm is given in reference.[10]

6.2 The governing equations

With excluded volume interactions described by the quadratic potential (66), the diffusion equation (1) becomes linear in the bead-connector vector. As a result, the diffusion equation is exactly satisfied by a Gaussian distribution (41). In Fixman's theory therefore, a tractable model is obtained not by approximating the distribution function, as in the case of the Gaussian approximation, but by introducing the quadratic potential (66).

While $\psi(\boldsymbol{Q}, t)$ is a Gaussian both in the Gaussian approximation and in Fixman's theory, the second moment which completely determines these distributions is different in the two cases. In Fixman's theory, the non-dimensional second moment $\langle \boldsymbol{Q}^*\boldsymbol{Q}^*\rangle$ is governed by the equation,

$$\frac{d}{dt^*}\langle \boldsymbol{Q}^*\boldsymbol{Q}^*\rangle = \boldsymbol{\kappa}^*\cdot\langle \boldsymbol{Q}^*\boldsymbol{Q}^*\rangle + \langle \boldsymbol{Q}^*\boldsymbol{Q}^*\rangle\cdot\boldsymbol{\kappa}^{*T} - \left[\,1 - \frac{z}{\alpha^2\sqrt{\det\langle \boldsymbol{Q}^*\boldsymbol{Q}^*\rangle}}\,\right]\langle \boldsymbol{Q}^*\boldsymbol{Q}^*\rangle + \mathbf{1} \tag{68}$$

Note that the second moment equation reduces to equation (67) at equilibrium.

The Giesekus expression for the stress tensor has the form,

$$\frac{\boldsymbol{\tau}^p}{nk_BT} = -\left[\,1 - \frac{z}{\alpha^2\sqrt{\det\langle \boldsymbol{Q}^*\boldsymbol{Q}^*\rangle}}\,\right]\langle \boldsymbol{Q}^*\boldsymbol{Q}^*\rangle + \mathbf{1} \tag{69}$$

As a result, the stress tensor in Fixman's theory, for any flow situation, may be obtained once equation (68) is solved for $\langle \boldsymbol{Q}^*\boldsymbol{Q}^*\rangle$.

It is clear from equation (69) that in Fixman's theory, as for $\mu > 0$ in the Gaussian approximation, rheological properties are affected both directly and indirectly by the presence of excluded volume.

As will be shown in the section below, at *steady state* in simple shear flow, the problem of solving the governing equation for the second moments (68), reduces to one of solving a single nonlinear algebraic equation. In the linear viscoelastic limit, however, analytical expressions for the various properties can be derived in the same manner as described earlier for the Gaussian approximation. Indeed, it can be shown that the linear viscoelastic properties are given by equations (53) and (54), where the quantities $\mathcal{H}$ and τ^* are now given by,

$$\mathcal{H} = 1 \quad ; \quad \tau^* = \alpha^2 \tag{70}$$

In steady simple shear flow, substituting equation (55) for $\langle \boldsymbol{Q}^* \boldsymbol{Q}^* \rangle$ and equation (10) for $\boldsymbol{\kappa}$, into the second moment equation (68), leads to the following equations for the components of $\langle \boldsymbol{Q}^* \boldsymbol{Q}^* \rangle$,

$$s_1 = (1 + 2\,\lambda_H^2 \dot{\gamma}^2\, s_2^2\,)\, s_2 \quad ; \quad s_3 = s_2 \quad ; \quad s_4 = \lambda_H\, \dot{\gamma}\, s_2^2$$

where, s_2 must satisfy the nonlinear algebraic equation,

$$s_2^{3/2} - s_2^{1/2} = \frac{\alpha(\alpha^2 - 1)}{\sqrt{1 + \lambda_H^2 \dot{\gamma}^2\, s_2^2}} \tag{71}$$

The normalised viscometric functions can be found by using the definitions (11), and the results above for the zero shear rate properties,

$$\frac{\eta_p}{\eta_{p,0}} = \frac{s_2}{\alpha^2} \quad ; \quad \frac{\Psi_1}{\Psi_{1,0}} = \frac{s_2^2}{\alpha^4} \quad ; \quad \Psi_2 = 0 \tag{72}$$

The nonlinear algebraic equation (71) is solved here with a Newton-Raphson scheme. The material functions predicted by Fixman's theory are compared with the predictions of the narrow Gaussian potential in the section below.

7 Results and Discussion

The predictions of rheological properties in simple shear flow, by the various theories for the excluded volume effect, are compared in this section. Predictions in the limit of zero shear rate are first considered below, and those at finite non-zero shear rates subsequently.

7.1 Zero shear rate properties

Figure 1 is a plot of $(\eta_{p,0}/\lambda_H\, n k_B T)$ versus μ for $z = 3$ and $z = 100$. The continuous curves are exact predictions obtained by numerical quadrature, while the

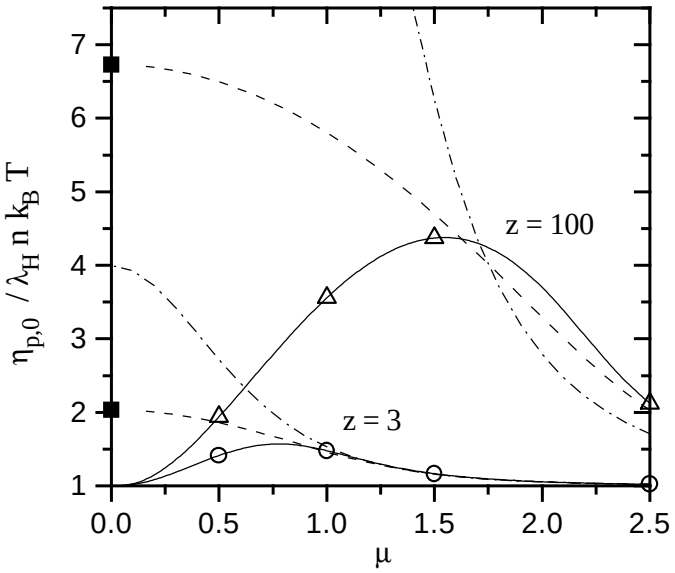

Figure 1: Non-dimensional zero shear rate viscosity versus the extent of excluded volume interaction μ, for two values of the strength of the interaction z. The continuous lines are exact predictions obtained by numerical quadrature, the triangles and circles are results of Brownian dynamics simulations, the dashed and the dot-dashed lines are the approximate predictions of the Gaussian approximation, and the first order perturbation theory, respectively, and the filled squares are the predictions of Fixman's theory. The error bars in the Brownian dynamics simulations cannot be resolved within the line thickness.

triangles and circles are exact results of Brownian dynamics simulations carried out at equilibrium (without variance reduction) [see equation (31)]. The dashed lines are the predictions of the Gaussian approximation for the narrow Gaussian potential [*i.e.* equation (54), with τ^* and $\mathcal{H}$ given by equations (48) and (50), respectively], the dot-dashed curve is the prediction of the first order perturbation theory [*i.e.* equation (61) in the limit $\lambda_H\dot{\gamma} \to 0$], and the filled squares are the predictions of Fixman's theory [*i.e.* equation (54), with τ^* and $\mathcal{H}$ given by equations (70)]. The parameter μ does not enter into Fixman's theory, however, these values are plotted corresponding to $\mu = 0$, since the quadratic potential is used in Fixman's theory as an approximation for the δ-potential.

The first feature to be noticed in figure 1 is the reassuring closeness of the exact results obtained by using the retarded motion expansion and by Brownian dynamics simulations. The retarded motion expansion provides a means of validating the results of Brownian dynamics simulations.

In the limit $\mu \to 0$, and for large values of μ, the continuous curves and Brownian dynamics simulations reveal that, as expected, the exact predictions of the narrow Gaussian potential tend to the z-independent θ-solvent value, $(\eta_{p,0}/\lambda_H\, nk_BT) = 1$. This implies, as pointed out earlier, that the use of a δ-function potential to represent excluded volume interactions does not lead to any change in the zero shear rate viscosity prediction. On the other hand, figure 1 seems to suggest that a finite

range of excluded volume interaction is required to cause a change from the θ-solvent value. Away from these limits, at non-zero values of μ, the narrow Gaussian potential predicts an increase in the value of zero shear rate viscosity. The existence of shear thinning in good solvents can be attributed to this increase. This follows from the fact that at high shear rates, as the effect of the excluded volume interaction diminishes, the viscosity is expected to return to its θ-solvent value. We shall see later that this expectation is indeed justified.

The dashed lines in figure 1 indicate that in the limit of zero shear rate, for a given value of z, the Gaussian approximation is reasonably accurate above a certain value of μ. This limiting value of μ appears to be smaller for smaller values of z. A similar behavior is also observed with regard to the prediction of the zero shear rate first normal stress difference (see figure 2). Thus it appears that the exact configurational distribution function $\psi(\boldsymbol{Q}, t)$ becomes increasingly non-Gaussian as the narrow Gaussian potential becomes narrower, and as the strength of the excluded volume interaction becomes larger.

For the large values of z considered in figure 1, results obtained with the first order perturbation expansion in z cannot be expected to be accurate. It is clear from the dot-dashed lines that the perturbation expansion results deviate significantly from exact results for small values of μ. However, they become increasingly accurate as μ increases, for a given value of z. This can be understood by considering equation (61), which indicates that in the limit $\lambda_H \dot{\gamma} \to 0$, the first order correction to the θ-solvent value increases as z increases, but decreases as μ increases.

As μ increases from zero, values of the zero shear rate viscosity predicted by the Gaussian approximation, approach the exact values more rapidly than the predictions of the first order perturbation theory, for a given value of z. The Gaussian approximation is a non-perturbative approximation—however, it was shown in section 5.4, to be exact to first order in z. One way to understand this is to consider the Gaussian approximation to consist of an infinite number of higher order terms, whose nature is unknown. In this sense, it is an *uncontrolled* approximation, which remains accurate at values of z and μ, where the first order perturbation expansion becomes inaccurate. As will be seen shortly, these remarks apply also to the results obtained at finite shear rate.

The difference in the prediction of the zero shear rate viscosity by Fixman's theory and by the narrow Gaussian potential is evident in figure 1. It is also worth noting that, although the relaxation weight and the relaxation time are different in Fixman's theory and in the Gaussian approximation for $\mu = 0$, they lead to the same prediction of the zero shear rate viscosity. This is, however, not true for the zero shear rate first normal stress difference. The ratio $U_{\Psi\eta}$, defined by,[15]

$$U_{\Psi\eta} = \frac{n k_B T \Psi_1}{\eta_p^2} \tag{73}$$

is equal, in the zero shear rate limit, to $(2/\alpha^2)$ in the Gaussian approximation, while it has a constant value of 2 in Fixman's theory.

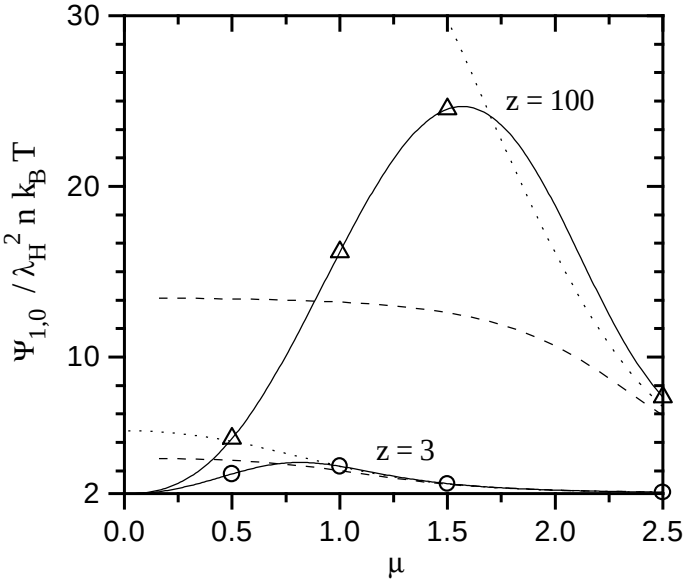

Figure 2: Non-dimensional zero shear rate first normal stress difference versus μ, for two values of z. The continuous lines are exact predictions obtained by numerical quadrature, the triangles and circles are results of Brownian dynamics simulations, the dashed lines are approximate predictions using the Gaussian approximation, and the dotted lines are approximate predictions using the uniform expansion model. The error bars in the Brownian dynamics simulations cannot be resolved within the line thickness.

Both the uniform expansion model and the Gaussian approximation use Gaussian distributions in order to evaluate averages. However, the uniform expansion model uses different Gaussian distributions for different equilibrium averages, such that the best approximation is obtained. While this does not lead to any difference in the prediction of the zero shear rate viscosity by the two approximations, figure 2 reveals that, at small enough values of μ, there is a significant difference in the prediction of the zero shear rate first normal stress difference. Clearly, the uniform expansion model continues to be a reasonable approximation for values of μ at which the Gaussian approximation is no longer accurate. However, even the uniform expansion model leads to a poor approximation at sufficiently small values of μ.

In the discussion of the equilibrium perturbation expansion in section 5.1.2, it was pointed out that, in principle, the equilibrium moment q_1 can be obtained for any non-zero value of μ, provided that enough numbers of terms in the series for the quantities S_0 and S_1, are summed [see equations (37)]. Figure 3 displays the sum S_0, for different numbers of summed terms in the perturbation expansion, as a function of μ, for $z = 3.0$. Exact results are obtained by noting that $S_0 = \sqrt{2/\pi}\, I_0$, and evaluating I_0 by numerical quadrature. Clearly, more terms of the expansion are required for convergence as μ decreases. The terms of the series, which are alternating in sign, keep increasing rapidly in magnitude, until n is approximately $> (z/\mu^3)$, before they begin to decrease. Therefore, as z increases, or as μ decreases,

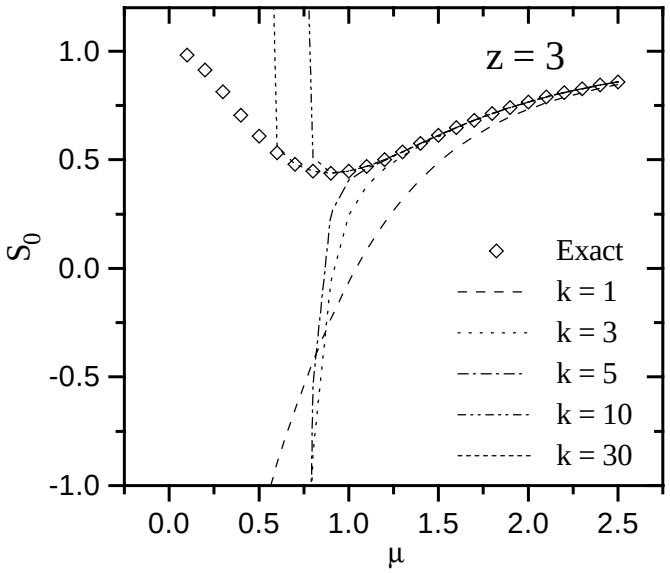

Figure 3: The sum S_0 versus μ, for different numbers of summed terms k in the perturbation expansion [see equation (37)]. The exact results are obtained by numerical quadrature.

more and more terms are required for the sum to converge. Above a threshold value of (z/μ^3) however, it becomes impossible to evaluate S_0 since the round-off errors due to the summation of large numbers makes the perturbation expansion numerically useless. A similar problem is also encountered while evaluating the sum S_1. In short, the hope of extrapolating finite μ results to the limit $\mu = 0$, cannot be realised. Therefore, in the case of Hookean dumbbells, one cannot obtain equilibrium moments for a delta function excluded volume potential by using a narrow Gaussian potential and considering a perturbation expansion in the limit $\mu \to 0$.

7.2 Steady state viscometric functions

The results of Brownian dynamics simulations (without variance reduction) displayed in figure 4 reveal that the dependence of the viscosity and the first normal stress difference on μ, at a value of the non-dimensional shear rate $\lambda_H\dot{\gamma} = 0.3$, is similar in shape to the dependence observed in the limit of zero shear rate. At small and large values of μ the material functions tend to the θ-solvent value, and exhibit a maximum at some value in between. Since, even at this non-zero value of shear rate, it appears that the viscosity and the first normal stress difference remain at their θ-solvent values for $\mu = 0$, it implies that the use of a δ-potential to represent excluded volume interactions would not predict any shear thinning. On the other hand, as we shall see subsequently, a quadratic potential does predict substantial shear thinning. At $\lambda_H\dot{\gamma} = 0.3$, the Gaussian approximation seems to be accurate above roughly the same values of μ as were observed in the limit of zero shear rate.

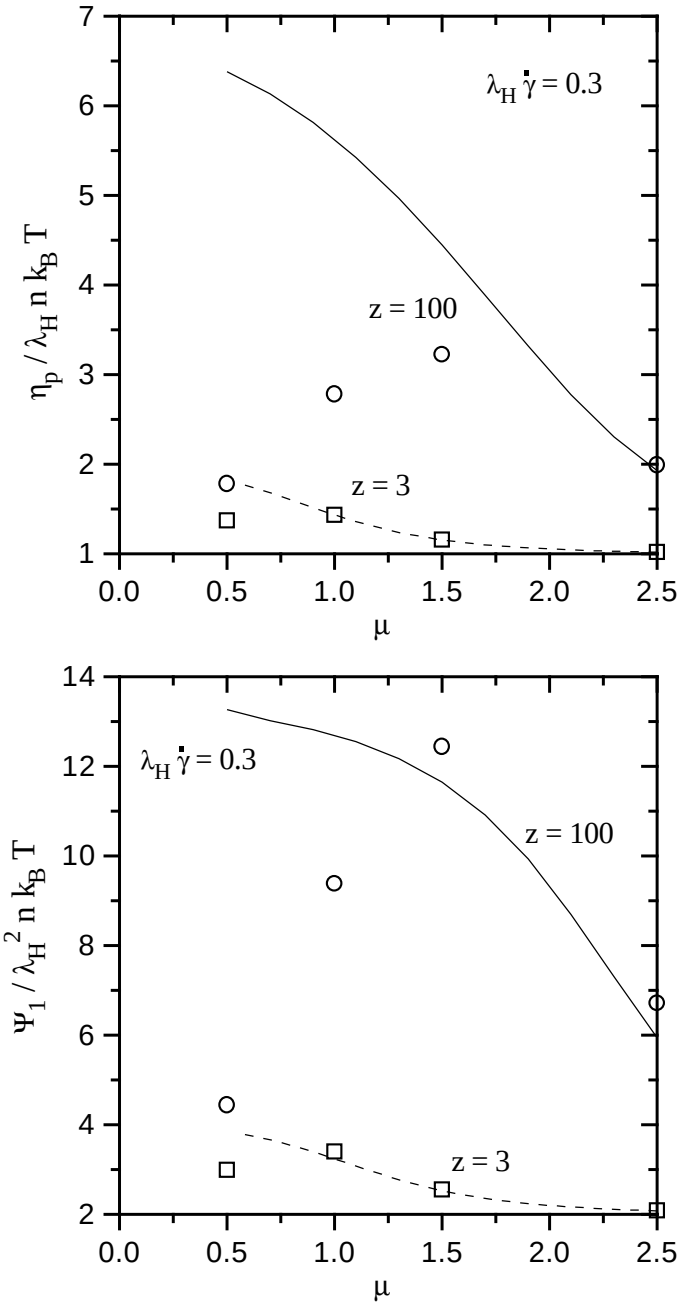

Figure 4: Non-dimensional viscosity and first normal stress difference versus μ for two values of z, at a non-dimensional shear rate $\lambda_H \dot{\gamma} = 0.3$. The squares and circles are results of Brownian dynamics simulations, and the dashed and continuous lines are the predictions of the Gaussian approximation, for $z = 3$ and $z = 100$, respectively. The error bars in the Brownian dynamics simulations cannot be resolved within the line thickness.

Figures 5 and 6 are plots of non-dimensional viscosity and first normal stress difference versus the non-dimensional shear rate $\lambda_H \dot{\gamma}$. Figure 5 displays the dependence of these viscometric functions on the parameter μ, for a fixed value of $z = 0.1$, while

figure 6 displays the dependence on the parameter z, for a fixed value of $\mu = 2.5$. The prediction of shear thinning for non-zero values of μ is apparent, and our earlier expectation in this direction is justified. In particular, the predictions of Brownian dynamics simulations, the Gaussian approximation, and the first order perturbation theory tend to θ-solvent values at high shear rates.

Shear thinning, which is seemingly physically meaningful, is also predicted, as can be seen from figure 5, by both the Gaussian approximation and the first order perturbation theory, for $\mu = 0$. This corresponds to a δ-function excluded volume potential, and is clearly an artifact of the perturbation expansion, since rigorous calculations indicate a trivial result. It remains to be seen if the situation is different in the limit of long chains.

For small enough values of z, and large enough values of μ, the results of the Gaussian approximation, and the first order perturbation expansion, agree exceedingly well with the exact results of Brownian dynamics simulations. Indeed, as $\lambda_H \dot{\gamma}$ increases for fixed values of z and μ, both the Gaussian approximation, and the first order perturbation expansion become increasingly accurate. In particular, if both the approximations are accurate at zero shear rate, they continue to remain accurate at non-zero shear rates. This can be understood in the case of the first order perturbation expansion by considering equations (61) and (62). Clearly, the departure from the θ-solvent values decreases as $\lambda_H \dot{\gamma}$ increases. This is inline with the intuitive expectation of decreasing excluded volume interactions with increasing shear rate.

For a fixed value of the shear rate $\lambda_H \dot{\gamma}$, as z increases, or μ decreases, the predictions of the Gaussian approximation and the first order perturbation expansion become increasingly inaccurate, with the first order perturbation expansion breaking down before the Gaussian approximation. This can be expected, since the Gaussian approximation—being exact to first order in z—is at least as accurate as the first order perturbation expansion.

The two different Brownian dynamics simulation algorithms mentioned in section 5.2 were used to obtain the data in figures 5 and 6. While the algorithm with variance reduction was used for shear rates upto $\lambda_H \dot{\gamma} = 0.1$, the algorithm without variance reduction was used at higher shear rates. With regard to the results obtained by variance reduction, it was found that the variance was typically reduced by a factor of five to ten by the parallel equilibrium simulation subtraction procedure. While the magnitude of the reduced variance was relatively independent of shear rate for the viscosity, it decreased with increasing shear rate for the first normal stress difference. The time to reach steady-state, from start-up of flow, was roughly ten relaxation times for $z = 0.1$, $z = 3$ and $z = 30$, and roughly fifteen relaxation times for $z = 100$. Rheological properties in the two parallel simulations remained correlated during the time required to reach steady-state, and as a result the present technique proved adequate for the purpose of variance reduction.

We have seen earlier—in figure 1—that both Fixman's theory, and the Gaussian approximation for $\mu = 0$, lead to identical values for the zero shear rate viscosity.

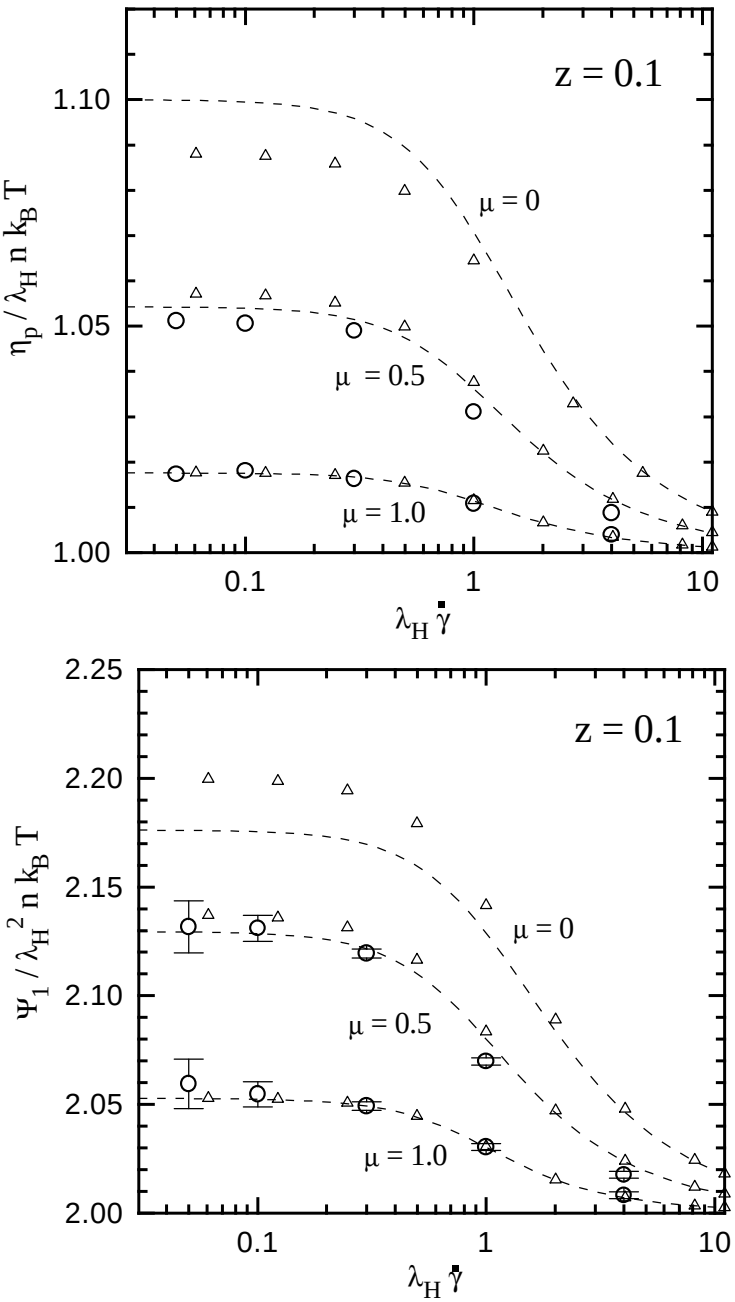

Figure 5: Non-dimensional viscosity and first normal stress difference versus non-dimensional shear rate $\lambda_H \dot{\gamma}$, for three values of μ at $z = 0.1$. The circles are results of Brownian dynamics simulations, the dashed lines are the predictions of the Gaussian approximation, and the triangles are the predictions of the first order perturbation expansion. In the viscosity plot, the error bars in the Brownian dynamics simulations are smaller than the size of the symbols.

This coincidence is, however, restricted to the limit of zero shear rate. At non-zero shear rates, as can be seen from figure 7, there is considerable divergence between the predictions of the two theories.

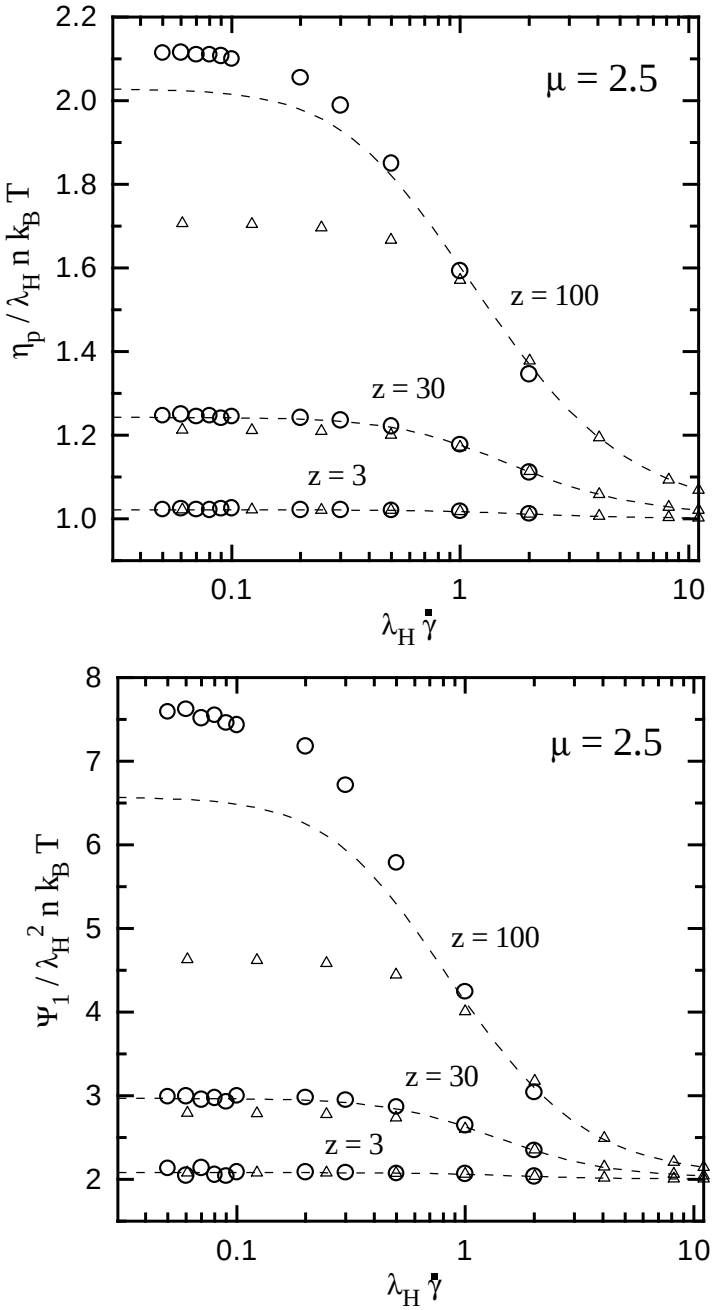

Figure 6: Non-dimensional viscosity and first normal stress difference versus $\lambda_H \dot{\gamma}$ for three values of z, at $\mu = 2.5$. The symbols are as indicated in the caption to figure 5. The error bars in the Brownian dynamics simulations are smaller than the size of the symbols.

Fixman's theory for dumbbells, though differing considerably from the narrow Gaussian potential in terms of its predictions of rheological properties, has the appealing aspect that it captures some of the *universal* features of the behavior of good solvents—which can only be expected from bead-spring chain theories in the limit of a large number of beads. We have seen this universal behavior earlier

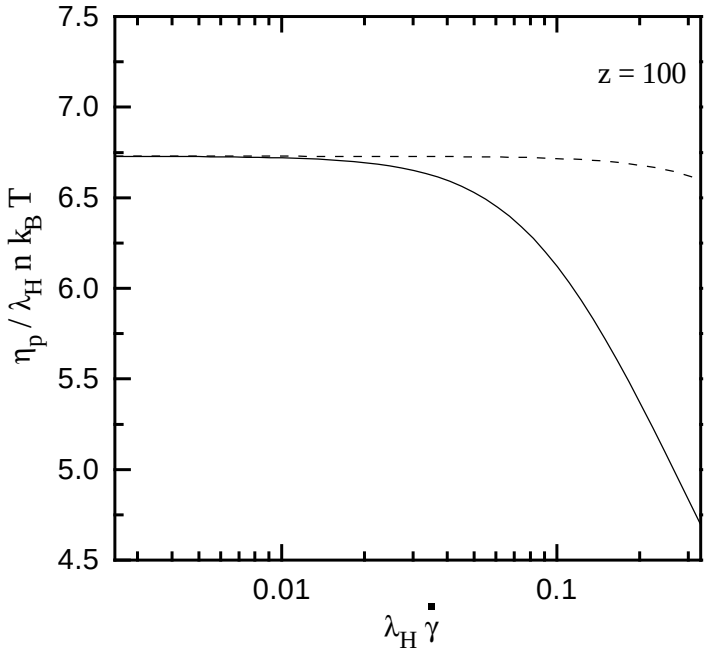

Figure 7: Non-dimensional viscosity versus non-dimensional shear rate for $z = 100$. The continuous line is the prediction of Fixman's theory, and the dashed line is the prediction of the Gaussian approximation for $\mu = 0$.

in the correct prediction of the end-to-end distance scaling, and in the parameter free nature of the ratio $U_{\Psi\eta}$. Figure 8 displays the prediction by Fixman's theory of the reduced variable $(\eta_p/\eta_{p,0})$ versus the non-dimensional shear rate $\beta = \lambda_p\dot{\gamma}$, where, $\lambda_p = (\,[\eta]_0\, M\, \eta_s/N_{\rm A}\, k_{\rm B}\, T\,)$, is a characteristic relaxation time. Here, $[\eta]_0$ is the zero shear rate intrinsic viscosity, M is the molecular weight and $N_{\rm A}$ is Avagadro's number. For dilute solutions one can show that, $\beta = \eta_{p,0}\,\dot{\gamma}/n\,k_{\rm B}\,T$. The figure clearly reveals that as $z \to \infty$, the curves for different values of z overlap. Therefore, in this respect also, Fixman's theory mimics the universal behavior expected of long chains. The source of this behavior can be understood by examining equation (71). In the limit of $\alpha \gg 1$, one can show that $s_2 = [\alpha^6\,(\lambda_H\dot{\gamma})^{-2}]^{1/5}$. As a result, $(\eta_p/\eta_{p,0}) = [\alpha^2\,\lambda_H\dot{\gamma}]^{-2/5}$ —leading to the observed scaling. At small values of $\lambda_H\dot{\gamma}$, $(\eta_p/\eta_{p,0}) \to 1$. One can therefore construct the analytical expression,

$$\frac{\eta_p}{\eta_{p,0}} = (1 + \alpha^4\lambda_H^2\dot{\gamma}^2)^{-1/5} \tag{74}$$

and expect it to be accurate at very small and large values of β. The dot-dashed curve in figure 8 shows that equation (74) is accurate over a fairly wide range of β.

The universal behavior discussed above is not exhibited by the Gaussian approximation. The reason for this can be easily understood in the limit $\mu \to 0$, where, the second moment equation (42) reduces at steady-state to a non-linear algebraic equation. Indeed, one can show that for $\alpha \gg 1$, $(\eta_p/\eta_{p,0}) = [1 + \lambda_H^2\dot{\gamma}^2]^{-1/5}$. As a result, the normalised material functions do not collapse onto a single curve when

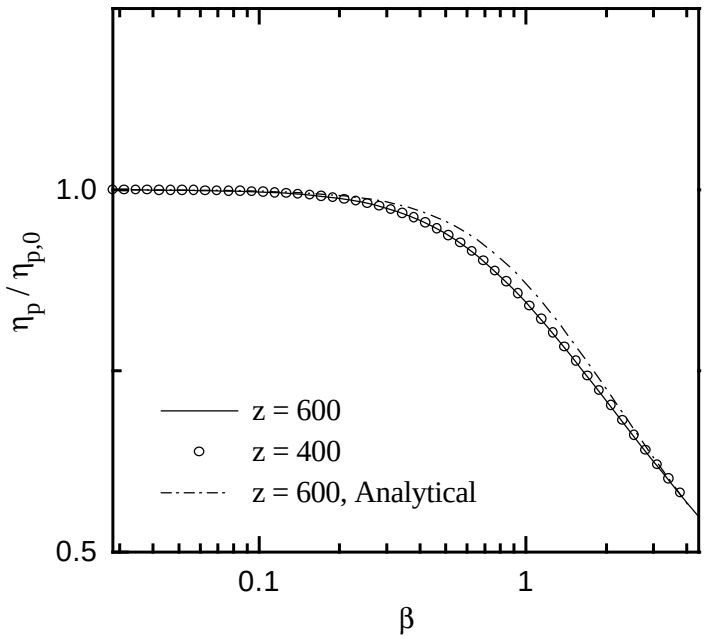

Figure 8: Reduced viscosity versus reduced shear rate predicted by Fixman's theory for large values of z. The continuous line and circles are obtained numerically, while the dot-dashed line is obtained with the analytical expression (74).

plotted versus β. It is, however, not realistic to expect a dumbbell model to exhibit universal features, and the real verification of universal behavior requires the development of a theory for long bead-spring chains.

The non-dimensional ratio $U_{\Psi\eta}$ [see equation (73)] has a constant value of two, independent of shear rate, for Hookean dumbbells in θ-solvents, and in Fixman's theory for good solvents. Figure 9 displays the predictions of $U_{\Psi\eta}$ by the narrow Gaussian potential, obtained by Brownian dynamics simulations, the Gaussian approximation, and the following first order perturbation expansion (which can be derived from equations (61) and (62)),

$$U_{\Psi\eta} = 2 - 2\,z\,\frac{1+\lambda_H^2\dot{\gamma}^2}{\sqrt{1+\mu^2}\,\Delta^{3/2}} \tag{75}$$

where, Δ has been defined below equation (62). Since a logarithmic scale has been chosen for the shear rate axis, it is difficult to represent the zero shear rate value of $U_{\Psi\eta}$. However, since it is very nearly constant at low values of shear rate, the zero shear rate value is represented in figure 9 by the filled circles on the y-axis. All the data in figure 9 have the same trend of remaining nearly constant at low shear rates, and approaching asymptotically the value of two at high shear rates. In the case of the first order perturbation expansion, this can be understood by considering equation (75) in the limit $\lambda_H\dot{\gamma} \to \infty$.

The dependence of the mean squared end-to-end distance $\langle Q^{*2}\rangle$ on $\lambda_H\dot{\gamma}$ is revealed in Figure 10. The circles and triangles are the results of Brownian dynamics

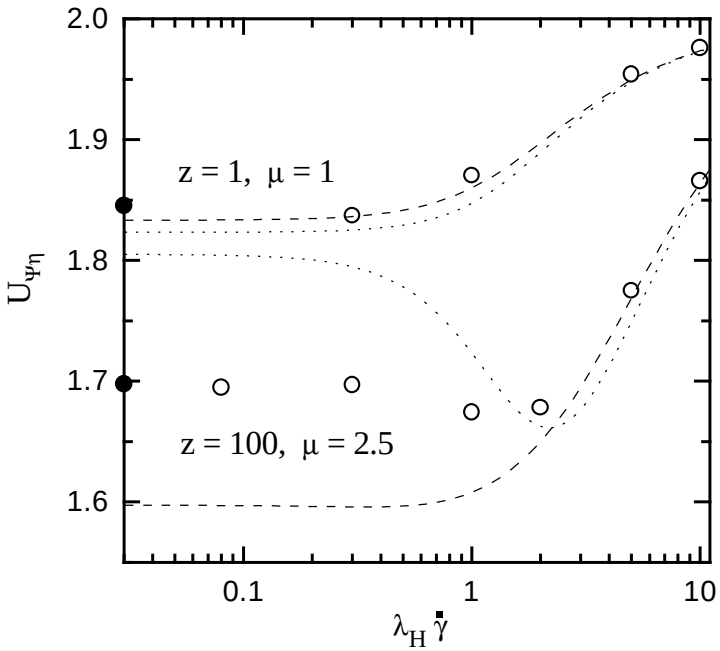

Figure 9: The ratio $U_{\Psi\eta}$ [see equation (73)] versus $\lambda_H\dot{\gamma}$. The circles are results of Brownian dynamics simulations, the dashed lines are the predictions of the Gaussian approximation, and the dotted lines are the predictions of the first order perturbation expansion. The filled circles on the y-axis represent zero shear rate values of $U_{\Psi\eta}$ obtained by equilibrium simulations. The error bars in the Brownian dynamics simulations are smaller than the size of the symbols.

simulations obtained with the algorithm without variance reduction. The dotted and dashed lines are plots of the following expression,

$$\langle Q^{*2}\rangle = 3 + 2\,\lambda_H^2\dot{\gamma}^2 + \frac{z}{\sqrt{1+\mu^2}\,\Delta^{3/2}}\left[3(1+\mu^2) + (5+6\mu^2)\,\lambda_H^2\dot{\gamma}^2 + 2\,\lambda_H^4\dot{\gamma}^4\right] \quad (76)$$

obtained from the first order perturbation expansion, and the continuous line is the well known result for a theta solvent,[5] $\langle Q^{*2}\rangle = 3 + 2\,\lambda_H^2\dot{\gamma}^2$. Interestingly, the effect of excluded volume interactions on swelling increases with increasing shear rate. In the case of the first order perturbation expansion—which appears to be accurate for $z = 3$, but not for $z = 30$—this can be understood by noting, in the expression above, that the term representing the correction to the theta solvent result due to the presence of excluded volume increases as the shear rate increases.

8 Conclusions

The use of a narrow Gaussian potential, to describe the excluded volume interactions between the beads of a Hookean dumbbell model, leads to the prediction of swelling and shear thinning for relatively small non-zero values of the extent of interaction

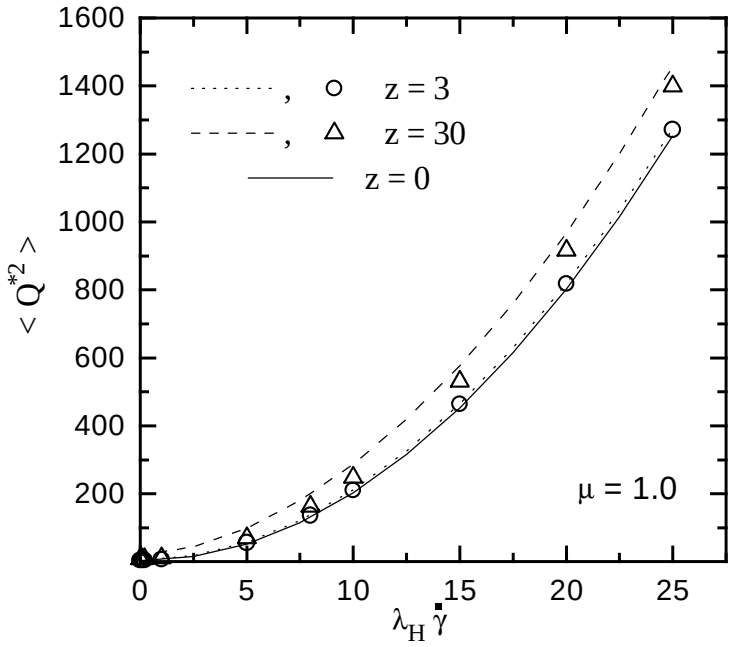

Figure 10: Non-dimensional mean squared end-to-end vector versus non-dimensional shear rate $\lambda_H\dot{\gamma}$, for two values of z at $\mu = 1$. The circles and triangles are results of Brownian dynamics simulations, the dotted and dashed lines are the predictions of the first order perturbation expansion, and the continuous line is the analytical solution for a theta solvent. The error bars in the Brownian dynamics simulations are smaller than the size of the symbols.

μ. This is essentially caused by an increase in the magnitude of the equilibrium moments relative to their θ-solvent values. A delta function description of the excluded volume potential, on the other hand, is found to predict neither swelling nor shear thinning for Hookean dumbbells.

For a given strength of the excluded volume interaction z, the Gaussian approximation is found to be reasonably accurate for values of μ larger than some threshold value. The behavior of the Gaussian approximation can be understood by comparing its predictions with those of a first order perturbation expansion in z, since it is shown here to be exact to first order in z. The perturbation expansion reveals that the departure of the viscometric functions from their θ-solvent values increases with increasing z, but decreases with increasing μ, and increasing shear rate $\lambda_H\dot{\gamma}$.

The use of a quadratic potential in Fixman's theory leads to the prediction of viscometric functions which are considerably different from those of the narrow Gaussian potential. However, Fixman's theory for dumbbells reproduces a number of universal features observed in good solvents.

Acknowledgement

Support for this work through a grant III. 5(5)/98-ET from the Department of

Science and Technology, India, to J. Ravi Prakash is acknowledged. Part of this work was carried out while JRP was a participant in the research programme *Jamming and Rheology* at the Institute for Theoretical Physics, University of California, Santa Barbara, USA. JRP would also like to thank the non-linear dynamics group at IIT Madras for providing the use of their computational facility.

References

(1) Ahn, K. H.; Lee, S. J. *J. Non-Newtonian Fluid Mech.* **1992**, *43*, 143; Ahn, K. H.; Schrag, J. L.; Lee, S. J. *J. Non-Newtonian Fluid Mech.* **1993**, *50*, 349.

(2) Andrews, N. C.; Doufas, A. K.; McHugh, A. J. *Macromolecules* **1998**, *31*, 3104.

(3) Arfken, G. *Mathematical Methods for Physicists,* 3rd edn.; Academic Press: Boston, 1985.

(4) Bird, R. B.; Armstrong, R. C.; Hassager, O. *Dynamics of Polymeric Liquids. Fluid Mechanics,* 2nd edn.; Wiley-Interscience: New York, 1987; Vol. 1.

(5) Bird, R. B.; Curtiss, C. F.; Armstrong, R. C.; Hassager, O. *Dynamics of Polymeric Liquids. Kinetic Theory,* 2nd edn.; Wiley-Interscience: New York, 1987; Vol. 2.

(6) Buck, R. C. *Advanced Calculus*; McGraw-Hill: New York, 1978.

(7) des Cloizeaux, J.; Jannink, G. *Polymers in Solution, Their Modelling and Structure*; Oxford University Press: Oxford, 1990.

(8) Doi, M.; Edwards, S. F. *The Theory of Polymer Dynamics*; Oxford University Press: Oxford, 1986.

(9) Fixman, M. *J. Chem. Phys.* **1966**, *45*, 785; **1966**, *45*, 793.

(10) Larson, R. G. *Constitutive Equations for Polymer Melts and Solutions*; Butterworths: Boston, 1988.

(11) Press, W. H.; Teukolsky, S. A.; Vetterling, W. T.; Flannery, B. P. *Numerical Recipes in FORTRAN*, 2nd edn.; Cambridge University Press: Cambridge, 1992.

(12) Öttinger, H. C. *J. Non-Newtonian Fluid Mech.* **1987**, *26*, 207.

(13) Öttinger, H. C.; Rabin, Y. *J. Non-Newtonian Fluid Mech.* **1989**, *33*, 53.

(14) Öttinger, H. C. *Phys. Rev.* **1989**, *A40*, 2664.

(15) Öttinger, H. C. *Stochastic Processes in Polymeric Fluids*; Springer: Berlin, 1996.

(16) Prakash, J. R. 'The Kinetic Theory of Dilute Solutions of Flexible Polymers: Hydrodynamic Interaction'. In *Advances in the Flow and Rheology of Non-Newtonian Fluids*; Siginer, D.A.; Kee, D.D.; Chhabra, R.P., Eds.; Rheology Series; Elsevier Science; In press.

(17) Schieber, J. D.; *J. Rheol.* **1993**, *37*, 1003.

(18) Wagner, N. J.; Öttinger, H. C. *J. Rheol.* **1997**, *41*, 757.

(19) Wedgewood, L. E. *Rheol. Acta* **1993**, *32*, 405.

(20) Yamakawa, H. *Modern Theory of Polymer Solutions*; Harper and Row: New York, 1971.

(21) Zylka, W.; Öttinger H. C. *J. Chem. Phys.* **1989**, *90*, 474.

(22) Zylka, W. *J. Chem. Phys.* **1991**, *94*, 4628.

(23) Zylka, W.; Öttinger H. C. *Macromolecules* **1991**, *24*, 484.

A The uniform expansion model

The equilibrium average of any quantity $X(\boldsymbol{Q})$ is given by,

$$\langle X \rangle_{\rm eq} = \mathcal{N}_{\rm eq} \int X(\boldsymbol{Q}) \, \exp\{ -\frac{3}{2b^2} Q^2 - E^* \} \, d\boldsymbol{Q} \tag{77}$$

where, $b^2 = 3(k_B T/H)$. By multiplying and dividing the integrand with the Gaussian distribution $\psi'_{\rm eq}(\boldsymbol{Q})$ [defined by equation (39)], and using the normalisation conditions on $\psi_{\rm eq}(\boldsymbol{Q})$ and $\psi'_{\rm eq}(\boldsymbol{Q})$, equation (77) can be rewritten in the form,

$$\langle X \rangle_{\rm eq} = \frac{\langle X(\boldsymbol{Q}) \, e^{-B(\boldsymbol{Q})} \rangle'_{\rm eq}}{\langle e^{-B(\boldsymbol{Q})} \rangle'_{\rm eq}} \tag{78}$$

where, $B(\boldsymbol{Q}) = (3/2)\,[\,(1/b^2) - (1/b'^2)\,]\,Q^2 + E^*$. For $\psi'_{\rm eq}(\boldsymbol{Q})$ to be a good approximation to $\psi_{\rm eq}(\boldsymbol{Q})$, $B(\boldsymbol{Q})$ must be small. On expanding $\exp(-B(\boldsymbol{Q}))$ in a Taylor's series, one can then write equation (78), to first order in $B(\boldsymbol{Q})$ as,

$$\langle X \rangle_{\rm eq} = \langle X \rangle'_{\rm eq} - \langle X\, B \rangle'_{\rm eq} + \langle X \rangle'_{\rm eq} \, \langle B \rangle'_{\rm eq} \tag{79}$$

If b' is chosen such that $\langle X\, B \rangle'_{\rm eq} = \langle X \rangle'_{\rm eq} \, \langle B \rangle'_{\rm eq}$, it then follows that $\langle X \rangle_{\rm eq}$ is well approximated by $\langle X \rangle'_{\rm eq}$.

The choice of b' that best optimises the approximation clearly depends on the quantity $X(\boldsymbol{Q})$ that is averaged. In our case we require averages of the quantities $X_{(m)} \equiv Q^{2m}$, $m = 1, 2, 3$. From the well known result for the moments of a Gaussian distribution,

$$\langle Q^{2m} \rangle'_{\rm eq} = \frac{2}{\sqrt{\pi}} \left[\frac{2{b'_{(m)}}^2}{3} \right]^m \Gamma(m + \frac{3}{2}) \tag{80}$$

where, $b'_{(m)}$ represents the value of b' corresponding to Q^{2m}. It follows that the optimum value of $b'_{(m)}$ is found by solving the following non-linear algebraic equation for $\alpha_{(m)}$,

$$(\alpha^2_{(m)} - 1)\, m + \frac{z}{[\alpha^2_{(m)} + \mu^2]^{3/2}} \left\{ \frac{\mu^{2m}}{[\alpha^2_{(m)} + \mu^2]^m} - 1 \right\} = 0 \tag{81}$$

where, $\alpha_{(m)} = b'_{(m)}/b$; $m = 1, 2, 3$. In terms of $\alpha_{(m)}$,

$$u_m = \alpha^{2m}_{(m)} \prod_{p=1}^{m} (2p + 1) \tag{82}$$